Journal of Mammalogy, 94(3):601–617, 2013

Intraspecific variability in *Lestoros inca* (Paucituberculata, Caenolestidae), with reports on dental anomalies and eruption pattern

GABRIEL M. MARTIN*

Consejo Nacional de Investigaciones Científicas y Técnicas (CONICET) and Laboratorio de Investigaciones en Evolución y Biodiversidad, Facultad de Ciencias Naturales Sede Esquel, Universidad Nacional de la Patagonia S.J.B. Esquel, Chubut, Argentina

* *Correspondent: gmartin_ar@yahoo.com*

Caenolestids are a group of poorly known South American marsupials with a restricted distribution in páramo and subpáramo environments of the Andes from Colombia and western Venezuela to Bolivia (represented by the genera *Caenolestes* and *Lestoros*), and in Valdivian rain forest in southern Chile and Argentina where a single species (*Rhyncholestes raphanurus*) lives. The Incan shrew opossum, *Lestoros inca*, lives in mountains of southern Peru and extreme northwestern Bolivia. Despite being common in trapping surveys, little is known of its cranial and dental intraspecific variability, tooth eruption pattern, and dental anomalies. The objective of this work was to analyze the intraspecific variability of *L. inca*, which includes an anatomical description of the skull and dentition and analysis of clinal variation, tooth eruption patterns, and dental anomalies. The eruption pattern found in *L. inca* confirms the sequence P3 → m4 → p3 → M4 as the general pattern for living paucituberculatans. Missing teeth between the procumbent incisor and the 2nd lower premolar are the most common anomaly found ($n = 14$, 20% of the analyzed specimens). Comparisons with other living caenolestids, lack of clinal variation and significant differences between populations support *L. inca* as a separate, clearly distinct species. The information presented herein can be used in anatomical and paleontological studies dealing with caenolestids in particular and marsupials in general and also provides a sound basis for anatomical inferences made from fossils.

Key words: craniodental anatomy, intraspecific variation, Marsupialia, Peruvian shrew opossum

DOI: 10.1644/12-MAMM-A-180.1

The family Caenolestidae (shrew opossums) includes 3 genera of living marsupials with a disjunct distribution along the Andes from northern Colombia–western Venezuela to northwestern Peru (*Caenolestes*), southern Peru to western Bolivia (*Lestoros*), and the temperate rain forests of Chile–Argentina (*Rhyncholestes*—Patterson 2007 [2008]). Caenolestids are the only living representatives of the once-diverse order Paucituberculata, which includes several specialized forms that had their maximum richness during the middle Tertiary (Abello 2007). Regarded as basal to the evolution of Paucituberculata (Marshall 1980), recent work has pointed out that living species might have a common ancestor, but they do not represent the basal radiation within the order as previously thought (Abello 2007; Goin et al. 2007).

Several studies have focused on different aspects of the dentition of living and fossil Paucituberculata (Marshall 1980; Goin et al. 2007, 2009; Martin 2008; but see Abello [2007] for a complete account on the works on this order), but most have analyzed a limited number of specimens for different reasons (e.g., limited number of specimens in fossil studies, limited access to collections of modern species, etc.). In this context, the study of larger series of individual species provides vital information on intraspecific variation, tooth eruption patterns, and other anatomical data important to both paleontologists and neontologists (e.g., cranial osteology, crest and cusp patterns, relative tooth sizes, dental anomalies, etc.).

The Incan shrew opossum, *Lestoros inca*, lives in páramo and subpáramo environments of southern Peru and extreme northwestern Bolivia (Myers and Patton 2007 [2008]). The species has been captured at different sites with variable ground cover, canopy cover, and slope, in isolated mountains from Ocobamba (Peru) to Llamachaque (Bolivia—Thomas 1917; Kirsch and Waller 1979; Anderson 1997; Brown 2004). Despite being relatively common in trapping surveys little is

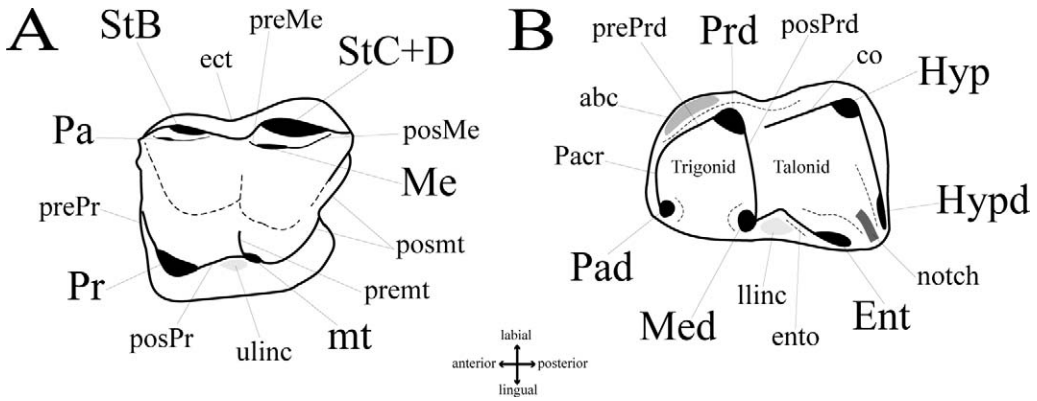

Fig. 1.—Schematic drawings in occlusal view of the A) 1st left upper and B) right lower caenolestid molars, depicting the nomenclature used in this study (modified from Abello 2007). Abbreviations: abc, anterobasal cingulum; co, cristida obliqua; ect, ectoflexus; Ent, entoconid; ento, entocristida; Hyp, hypoconid; Hypd, hypoconulid; llinc, lower lingual cingulum; Me, metacone; Med, metaconid; mt, metaconule; Pa, paracone; Pacr, paracristida; Pad, paraconid; Pr, protocone; Prd, protoconid; preMe, premetacrista; premt, premetaconular crest; prePr, preprotocrista; prePrd, preprotocristida; posMe, postmetacrista; posmt, postmetaconular crest; posPr, postprotocrista; posPrd, postprotocristida; StB, stylar cusp B; StC+D, stylar cusp C+D; ulinc, upper lingual cingulum.

known of the intraspecific variability of *L. inca* and other anatomical and ecological features.

In a craniometric study based on 47 specimens from a few localities, Bublitz (1987) proposed the genus *Lestoros* should not be separated from *Caenolestes* and included the species as *Caenolestes inca*. In the same work, the author separated the Peruvian forms into 2 syntopic species: *C. inca* and *C. gracilis*, but Timm and Patterson (2007 [2008]) rejected this arrangement. In another study, Luckett and Hong (2000) described the tooth eruption pattern and discussed dental homologies in extant and fossil caenolestids, but no information was given about *L. inca* because of a lack of subadult or juvenile specimens. The most comprehensive study to date on the systematics of living and extinct Paucituberculata (Abello 2007) included limited information on *L. inca*. My access to larger series and specimens from new localities allowed for a more comprehensive understanding of different aspects of the craniodental anatomy of *L. inca*, which is presented herein. This is done to provide information on the variability of the species that can be used in anatomical and paleontological studies dealing with caenolestids in particular and marsupials in general. Most paleontological studies deal with few specimens and, in many cases, it is difficult to get a glimpse of the variation of a fossil taxon. Therefore, a better understanding of the variability of characters in the living species provides a sound basis for anatomical inferences made in fossils.

The main objective of this work was to provide new information on aspects of the intraspecific variability and craniodental anatomy of *L. inca*. This was done through the following: analysis of intraspecific sexual differences within localities; analysis of differences between localities; redescription of the skull and teeth of *L. inca* and its intraspecific variability; and a report on tooth eruption pattern and dental anomalies. The main differences in craniodental characters between living caenolestids also are presented.

Materials and Methods

External measurements were taken from skin tags or field catalogs, and include total length (TTL), head–body length (HBL), tail length (TL), ear length (E), and hind-foot length (F). When HBL was not provided, it was calculated by subtracting TL from TTL. When TTL was not provided, it was calculated by adding HBL to TL.

Cranial anatomy follows Osgood (1921), except for the palate, for which I follow Voss and Jansa (2003). Specimen USNM 194395 from Torontoy is a topotype (see Thomas 1917) and was chosen to describe molar morphology in detail because of its low degree of tooth wear. Dental nomenclature follows Abello (2007) and is presented in Fig. 1. Dental homologies follow Luckett and Hong (2000). Upper and lower dentition are designated by uppercase and lowercase letters, respectively. Therefore, teeth found in adult dentition of caenolestids are designated as follows: upper and lower incisors, I1–4 and i1–3 (from anterior to posterior); canines, C1 and c1; premolars, dP1–2 and dp1–2, and P3 and p3; and molars, M1–4 and m1–4. The single functional deciduous tooth in each jaw quadrant, when referenced, is designated dP3 or dp3. As described by Luckett and Hong (2000), the first 2 upper and lower premolars are considered unreplaced deciduous teeth. Lower teeth between the procumbent incisor (numerical i1, but see Luckett and Hong [2000] for a discussion on 1st lower incisor's homologies) and the 1st identifiable lower premolar (dp2) are referred to as "incisor-like teeth." I took 33 measurements of crania, mandibles, and teeth from adult specimens (as indicated by completed tooth eruption): greatest skull length (GSL); zygomatic breadth (ZB); palatine length (PL); palate width at canines (CW); palate width at P3 (PWP3); palate width at M1 (PWM1); palate width at M3 (PWM3); interorbital constriction (LINOR); nasal length (NSL); braincase width (BW); condylobasal length (CBL); distance between bullae (BB); mandibular width (MW); mandibular height at p3 (MHp3); mandibular height at m3

(MHm3); length from the anteriormost point of the 1st upper premolar to the posteriormost point of the last upper molar (dP1–M4); length from the anteriormost point of the 1st upper premolar to the posteriormost point of the 3rd upper molar (dP1–M3); length from the anteriormost point of the 3rd upper premolar to the posteriormost point of the last upper molar (P3–M4); length from the anteriormost point of the 3rd upper premolar to the posteriormost point of the 3rd upper molar (P3–M3); length from the anteriormost point of the 3rd lower premolar to the posteriormost point of the last lower molar (p3–m4); length from the anteriormost point of the 3rd lower premolar to the posteriormost point of the 3rd lower molar (p3–m3); length from the anteriormost point of the 1st upper molar to the posteriormost point of the 3rd upper molar (M1–M3); length from the anteriormost point of the 1st upper molar to the posteriormost point of the last upper molar (M1–M4); length from the anteriormost point of the 1st lower molar to the posteriormost point of the 3rd lower molar (m1–m3); length from the anteriormost point of the 1st lower molar to the posteriormost point of the last lower molar (m1–m4); length from the anteriormost point of the 2nd lower premolar to the posteriormost point of the 3rd lower molar (dp2–m3); length from the anteriormost point of the 2nd lower premolar to the posteriormost point of the last lower molar (dP2–m4); length of 1st upper molar (LM1); width of 1st upper molar (WM1); length of 1st lower molar (Lm1); width of 1st lower molar (Wm1); length of 3rd upper molar (LM3); and width of 3rd upper molar (WM3).

Measurements of adult specimens were used to assess intraspecific variation, including possible sexual dimorphism. All measurements used in statistical analyses were converted to $\log_{10}$. A standard Bonferroni ($P = \alpha/n$) correction was used on *P*-values for the analyzed variables following Rice (1989) and Cerqueira and Lemos (2000): 0.01 and 0.002 for external measurements with *P*-values of 0.05 and 0.01; and 0.0015625 and 0.0003125 for craniodental variables with *P*-values of 0.05 and 0.01, respectively.

A 1-way analysis of variance (ANOVA) was performed to test for sexual dimorphism among specimens from localities with specimen numbers ≥ 6. Because of their proximity, and to increase the number of measured specimens, 2 sets of localities were pooled: Ocobamba–Cedrobamba–Torontoy and La Esperanza–Pillahuata.

A 1-way ANOVA was performed to test for differences between specimens of *L. inca* that were assigned by Bublitz (1987) to *C. inca* and *C. gracilis*. Apart from this, 3 principal component analyses were carried out to test for intraspecific dispersion and to include specimens from localities that could not be included in the ANOVAs because of small sample size: the external measurements (TTL, HBL, TL, E, and F); craniodental measurements (GSL, ZB, PL, PWP3, PWM1, PWM3, LINOR, NSL, BW, CBL, BB, dP1–M4, dP1–M3, P3–M4, P3–M3, p3–m4, p3–m3, M1–M3, M1–M4, m1–m3, m1–m4, dp2–m3, dp2–m4, LM1, WM1, Lm1, Wm1, LM3, and WM3); and only dental measurements (dP1–M4, dP1–M3, P3–M4, P3–M3, p3–m4, p3–m3, M1–M3, M1–M4, m1–m3, m1–m4, dp2–m3, dp2–m4, LM1, WM1, Lm1, Wm1, LM3, and WM3). I followed Cattell (1966) in selecting the number of principal components (PCs) for each analysis. The first 2 axes of each principal component analysis were regressed with latitude to test for clinal variation. Statistical analyses were performed using InfoStat (Di Rienzo et al. 2010). See Appendix I for specimen number, provenance, and sex.

Description of eruption patterns and function partially follows Luckett and Hong (2000), whereas description of dental anomalies follows Martin (2007).

Results

A total of 136 specimens of *L. inca* from several localities were analyzed in this study (Appendix I). The total number of specimens measured for each locality, mean, *SD*, minimum and maximum of each variable, and coefficient of variation are presented in Tables 1 and 2. One locality produced more than 35% of the specimens, whereas the other localities vary between 19% and ~5% (Tables 1 and 2; Appendix I). ANOVA for sexual dimorphism by locality is presented in Table 3. Significant differences were only found in external measurements from 3 localities: La Esperanza (with differences in TTL, HBL, TL, and F), Limacpunco (with differences in TTL, TL, and E), and Torontoy (with differences in F). ANOVA for sexual dimorphism within grouped localities is presented in Table 4. Significant differences again were only found on external measurements. Craniodental measurements provided the least within-group variation. ANOVA to test for differences between specimens assigned by Bublitz (1987) to *C. inca* and *C. gracilis* is presented in Table 5. No significant differences were found between these groups, supporting the notion of *L. inca* as a single species. Results of the 3 principal component analyses for external, craniodental, and dental measurements are presented in Tables 6, 7, and 8, respectively. The first 2 PCs explained 79%, 70%, and 74% of the total variance in each analysis, respectively. No significant trend was found when the first 2 PCs were regressed with latitude for any set of variables, indicating no evidence for clinal variation (external measurements: $n = 129$; PC1, $r^2 = 1.8\text{E}{-6}$, $F = 2.3\text{E}{-4}$, $P = 0.9888$; PC2, $r^2 = 1.10\text{E}{-9}$, $F = 1.3\text{E}{-7}$; $P = 0.9997$; craniodental measurements: $n = 49$; PC1, $r^2 = 7.7\text{E}{-6}$, $F = 3.7\text{E}{-4}$, $P = 0.9847$; PC2, $r^2 = 5.10\text{E}{-8}$, $F = 2.4\text{E}{-6}$, $P = 0.9988$; dental measurements: $n = 64$; PC1, $r^2 = 1.2\text{E}{-5}$, $F = 7.8\text{E}{-4}$, $P = 0.9778$; PC2, $r^2 = 2.3\text{E}{-6}$, $F = 1.5\text{E}{-4}$, $P = 0.9904$).

Character Descriptions, Intraspecific Variability, and Comparison with Other Caenolestids

Crania.—In dorsal view, nasals do not project beyond the anterior extension of premaxillae. They are mostly narrow throughout the proximal three-fourths of their extension, expanding in the distal one-fourth posterior to the contact point between the posteriormost extension and the

Table 1.—External and craniodental measurements of *Lestoros inca*. Total number of specimens (*n*), mean ($\bar{X}$), *SD*, minimum (min), and maximum (max) of each variable, and coefficient of variation (*CV*) are presented for each locality. Asterisks (*) indicate *CV* values higher than 7, following Bedian and Mossholder (2000). Variables are defined in the text.

	Torontoy		Cedrobamba		La Esperanza	
Variable	*n*	$\bar{X} \pm SD$ (min–max) *CV*	*n*	$\bar{X} \pm SD$ (min–max) *CV*	*n*	$\bar{X} \pm SD$ (min–max) *CV*
TTL	20	221.2 ± 10.5 (193–233) 4.74	18	217.89 ± 10.74 (202–233) 4.93	45	220.02 ± 9.39 (201–240) 4.27
HBL	21	102.95 ± 6.66 (90–120) 6.47	18	100.72 ± 8.13 (90–115) 8.07*	45	102.84 ± 6.89 (90–117) 6.7
TL	20	118.1 ± 8.7 (103–129) 7.36*	18	117.17 ± 7.62 (103–135) 6.5	45	117.18 ± 5.61 (103–130) 4.78
E	21	14.9 ± 0.4 (14–16) 2.93	18	14.81 ± 0.64 (14–16) 4.36	45	15.16 ± 0.80 (13–16) 5.26
F	21	23.07 ± 0.83 (22–25) 3.58	18	22.83 ± 0.66 (22–24) 2.91	45	23.51 ± 0.92 (21–25) 3.91
GSL	15	30.2 ± 0.8 (29.06–32.36) 2.82	12	29.41 ± 0.99 (27.97–31.70) 3.37	7	29.72 ± 0.44 (29.11–30.30) 1.48
ZB	16	14.15 ± 0.41 (13.49–15.19) 2.87	14	13.77 ± 0.49 (13.06–14.91) 3.54	7	13.92 ± 0.36 (13.36–14.43) 2.61
PL	17	16.81 ± 0.78 (15.52–18.69) 4.63	12	16.35 ± 0.75 (15.32–18.01) 4.59	7	16.69 ± 0.23 (16.38–17.09) 1.38
CW	20	3.91 ± 0.21 (3.61–4.34) 5.25	16	3.84 ± 0.22 (3.56–4.22) 5.68	7	3.78 ± 0.15 (3.58–3.96) 3.93
PWP3	20	6.30 ± 0.16 (5.79–6.55) 2.58	17	6.12 ± 0.23 (5.82–6.45) 3.68	7	6.24 ± 0.20 (5.92–6.48) 3.17
PWM1	20	6.79 ± 0.18 (6.32–7.26) 2.63	17	6.77 ± 0.23 (6.48–7.32) 3.38	7	6.86 ± 0.06 (6.78–6.93) 0.84
PWM3	20	7.40 ± 0.17 (6.99–7.70) 2.29	17	7.35 ± 0.18 (7.06–7.75) 2.41	7	7.46 ± 0.10 (7.26–7.59) 1.36
LINOR	20	7.31 ± 0.17 (7.06–7.70) 2.35	18	7.21 ± 0.16 (6.96–7.59) 2.2	7	7.23 ± 0.22 (6.83–7.57) 3.04
NSL	20	14.46 ± 0.83 (13.06–16.51) 5.76	17	14.37 ± 0.99 (12.98–16.28) 6.91	6	13.69 ± 0.38 (13.23–14.22) 2.8
BW	18	12.46 ± 0.32 (11.94–12.88) 2.55	18	12.29 ± 0.26 (11.84–12.73) 2.15	7	12.52 ± 0.10 (12.40–12.70) 0.76
CBL	16	27.06 ± 0.99 (25.91–29.49) 3.65	12	26.23 ± 1.23 (24.43–28.55) 4.7	7	26.43 ± 0.51 (25.91–27.38) 1.93
BB	18	5.52 ± 0.24 (5.11–6.05) 4.43	18	5.38 ± 0.27 (4.93–5.84) 4.94	7	5.43 ± 0.15 (5.26–5.61) 2.79
MW	20	0.95 ± 0.06 (0.84–1.07) 6.16	18	0.92 ± 0.06 (0.81–1.04) 6.32	7	0.96 ± 0.05 (0.89–1.04) 4.77
MHp3	20	2.37 ± 0.11 (2.13–2.57) 4.69	18	2.22 ± 0.18 (1.91–2.64) 7.99*	7	2.29 ± 0.10 (2.16–2.46) 4.55
MHm3	20	2.18 ± 0.17 (1.83–2.54) 7.65*	18	2.03 ± 0.17 (1.68–2.39) 8.44*	7	2.15 ± 0.08 (2.06–2.29) 3.52
dP1–M3	20	8.66 ± 0.31 (8.13–9.45) 3.58	18	8.68 ± 0.34 (8.10–9.42) 3.88	7	8.40 ± 0.21 (7.98–8.61) 2.53
dP1–M4	20	9.11 ± 0.34 (8.28–9.93) 3.76	17	9.11 ± 0.37 (8.53–9.80) 4.09	7	8.78 ± 0.16 (8.46–8.92) 1.82
P3–M3	20	6.19 ± 0.34 (5.72–6.86) 5.5	18	6.23 ± 0.32 (5.79–6.68) 5.13	7	5.99 ± 0.12 (5.77–6.12) 1.92
P3–M4	20	6.65 ± 0.38 (6.02–7.37) 5.77	17	6.65 ± 0.43 (6.05–7.24) 6.43	7	6.38 ± 0.15 (6.17–6.55) 2.36
M1–M3	20	4.93 ± 0.25 (4.62–5.38) 5.12	18	4.98 ± 0.21 (4.67–5.38) 4.2	7	4.73 ± 0.13 (4.57–4.88) 2.73
M1–M4	20	5.48 ± 0.26 (5.08–5.94) 4.8	17	5.49 ± 0.28 (5.08–5.94) 5.18	7	5.17 ± 0.19 (4.83–5.36) 3.77
LM1	20	1.78 ± 0.14 (1.52–2.01) 7.84*	18	1.82 ± 0.14 (1.63–2.03) 7.51*	7	1.68 ± 0.05 (1.60–1.75) 3.2
WM1	20	1.59 ± 0.07 (1.50–1.70) 4.23	18	1.6 ± 0.1 (1.4–1.7) 3.51	7	1.60 ± 0.04 (1.55–1.65) 2.33
LM3	20	1.55 ± 0.07 (1.40–1.73) 4.42	18	1.53 ± 0.08 (1.40–1.65) 4.94	7	1.48 ± 0.04 (1.42–1.52) 2.59
WM3	20	1.54 ± 0.07 (1.45–1.65) 4.38	18	1.47 ± 0.06 (1.40–1.55) 3.95	7	1.50 ± 0.05 (1.45–1.55) 3
dp2–m3	19	7.15 ± 0.40 (6.53–7.77) 5.64	18	7.06 ± 0.30 (6.48–7.49) 4.18	6	6.94 ± 0.13 (6.78–7.16) 1.9
dp2–m4	19	8.09 ± 0.43 (7.57–8.84) 5.35	18	8 ± 0.28 (7.42–8.41) 3.48	6	7.74 ± 0.20 (7.52–8.05) 2.62
m1–m3	20	5.18 ± 0.24 (4.85–5.72) 4.58	18	5.14 ± 0.24 (4.70–5.54) 4.59	7	5.04 ± 0.12 (4.88–5.23) 2.31
m1–m4	20	6.10 ± 0.28 (5.79–6.71) 4.61	18	6.09 ± 0.23 (5.66–6.48) 3.76	7	5.86 ± 0.18 (5.64–6.15) 3.08
p3–m3	20	5.94 ± 0.36 (5.56–6.58) 6.05	18	6.06 ± 0.42 (5.46–7.19) 6.97	7	5.79 ± 0.16 (5.61–6.10) 2.75
p3–m4	20	6.87 ± 0.41 (6.40–7.65) 5.89	18	6.78 ± 0.42 (5.72–7.39) 6.13	7	6.59 ± 0.23 (6.27–6.96) 3.44
Lm1	20	1.87 ± 0.08 (1.78–2.03) 4.06	18	1.85 ± 0.10 (1.57–2.01) 5.64	7	1.80 ± 0.02 (1.78–1.83) 0.97
Wm1	20	0.96 ± 0.07 (0.86–1.07) 6.89	18	0.95 ± 0.06 (0.81–1.04) 6.03	7	0.92 ± 0.04 (0.86–0.97) 3.8

posterodorsal spine of the premaxillae and the maxillae (Fig. 2). There, they expand (broaden) laterally at the antorbital vacuity and narrow after this, forming a U (or a wide W). Posteriorly, they extend to a point equal or subequal to the anteriormost extension of the orbits. Most specimens show open (unossified) antorbital vacuities of variable size and different extensions of the bones internally (Fig. 2). A few specimens (of both sexes) show completely ossified antorbital vacuities (e.g., USNM 194422, USNM 194419, USNM 194421, and USNM 194403; Fig. 2). This character is not related to the age of the specimens, because young individuals (those with little worn teeth such as USNM 194395) also may show almost completely ossified antorbital vacuities. Frontals extend anteriorly to a point dorsal to the medial part (ectoflexus) of M1, slightly anterior to the infraorbital foramen, and do not contact the dorsoposterior spine of the premaxillary bone. Posteriorly, the contact between frontals and parietals is almost straight in dorsal view, forming a transverse line to the anteroposterior axis of the skull, sometimes with a narrow posterior projection where the 4 bones contact. Parietals are mostly square with very little anterior development, and abut the supraoccipital bone to which they are fused in some specimens. *L. inca* does not have well-marked lambdoid crests; in only a few specimens (e.g., FMNH 75115 and FMNH 22439), mostly males, short lateral crests are developed between the supraoccipital and parietal bones and above the mastoid (sensu Osgood 1921).

In lateral view, the premaxillary bone extends posteriorly to a point anterior to the canine. Posterodorsally, the premaxillary spine is of variable length, extending in most specimens to a point between dP2 and P3 (e.g., USNM 194419, USNM 194427, and FMNH 75120) or above dP2 (e.g., FMNH 22439 and USNM 194433), with some specimens showing a more posteriorly extended pattern (e.g., anteromedial to P3; USNM

Table 2.—External and craniodental measurements of *Lestoros inca*. Total number of specimens (*n*), mean ($\bar{X}$), *SD*, minimum (min), and maximum (max) of each variable, and coefficient of variation (*CV*) are presented for each locality. Asterisks (*) indicate *CV* values higher than 7, following Bedian and Mossholder (2000). Variables are defined in the text.

	Limacpunco		Ocobamba		Pillahuata	
Variable	*n*	$\bar{X} \pm SD$ (min–max) *CV*	*n*	$\bar{X} \pm SD$ (min–max) *CV*	*n*	$\bar{X} \pm SD$ (min–max) *CV*
TTL	13	222.62 ± 13.45 (191–240) 6.04	6	216 ± 18.84 (193–236) 8.72*	24	217.08 ± 12.43 (193–245) 5.73
HBL	13	106.62 ± 8.10 (86–115) 7.6*	6	100.67 ± 8.09 (91–110) 8.04*	24	101.17 ± 8.22 (88–115) 8.13*
TL	13	116 ± 7 (105–127) 6.03	6	115.33 ± 13 (96–126) 11.27*	25	115.32 ± 6.85 (101–132) 5.94
E	13	15.38 ± 0.65 (14–16) 4.23	6	15 ± 1.26 (14–17) 8.43*	25	15.12 ± 0.83 (14–17) 5.51
F	13	24.08 ± 0.76 (23–25) 3.15	6	23 ± 1.41 (21–25) 6.15	25	23.48 ± 1 (21–25) 4.28
GSL	10	30.15 ± 1.09 (27.86–31.57) 3.6	3	29.71 ± 0.86 (28.98–30.66) 2.89	7	29.96 ± 0.69 (28.91–30.89) 2.30
ZB	10	14.05 ± 0.71 (12.65–14.99) 5.03	4	14.03 ± 0.81 (12.88–14.76) 5.77	7	13.99 ± 0.4 (13.51–14.73) 2.83
PL	10	17.08 ± 0.79 (15.44–18.11) 4.62	4	16.45 ± 0.44 (16–17.02) 2.67	7	16.77 ± 0.67 (15.85–17.7) 3.96
CW	10	3.92 ± 0.22 (3.56–4.14) 5.71	6	3.89 ± 0.11 (3.76–4.04) 2.71	7	3.90 ± 0.28 (3.43–4.22) 7.05*
PWP3	10	6.23 ± 0.30 (5.69–6.60) 4.76	6	6.17 ± 0.23 (5.92–6.40) 3.73	7	6.22 ± 0.20 (5.94–6.60) 3.23
PWM1	10	6.90 ± 0.34 (6.25–7.32) 4.98	6	6.79 ± 0.28 (6.50–7.11) 4.16	7	6.82 ± 0.18 (6.63–7.06) 2.60
PWM3	10	7.43 ± 0.30 (6.93–7.98) 4.02	6	7.37 ± 0.27 (7.01–7.80) 3.69	7	7.46 ± 0.19 (7.21–7.80) 2.53
LINOR	10	7.37 ± 0.26 (7.04–7.92) 3.57	6	7.45 ± 0.16 (7.16–7.59) 2.16	7	7.32 ± 0.25 (6.96–7.75) 3.38
NSL	10	14.59 ± 0.54 (13.31–15.11) 3.71	6	14.11 ± 0.37 (13.59–14.53) 2.62	6	14.07 ± 0.73 (13–14.88) 5.17
BW	10	12.60 ± 0.50 (11.71–13.31) 3.93	4	12.25 ± 0.63 (11.43–12.95) 5.14	7	12.55 ± 0.30 (12.09–12.95) 2.37
CBL	10	26.93 ± 1.18 (24.38–28.63) 4.39	3	26.54 ± 0.76 (25.98–27.41) 2.86	7	26.52 ± 0.91 (24.99–27.58) 3.44
BB	10	5.66 ± 0.17 (5.33–5.94) 3.09	4	5.49 ± 0.34 (5.08–5.92) 6.28	7	5.48 ± 0.19 (5.33–5.87) 3.47
MW	10	0.99 ± 0.09 (0.86–1.17) 9.45*	6	0.97 ± 0.14 (0.84–1.14) 14.35*	7	1.01 ± 0.10 (0.91–1.22) 10.2*
MHp3	10	2.37 ± 0.20 (2.03–2.64) 8.23*	6	2.26 ± 0.26 (1.96–2.67) 11.31*	7	2.36 ± 0.16 (2.16–2.59) 6.91
MHm3	10	2.25 ± 0.18 (2.06–2.51) 7.93*	6	1.99 ± 0.29 (1.52–2.29) 14.46*	7	2.24 ± 0.21 (2.06–2.67) 9.43*
dP1–M3	9	8.70 ± 0.24 (8.38–9.07) 2.78	6	8.75 ± 0.47 (8.10–9.53) 5.36	7	8.23 ± 0.18 (7.95–8.43) 2.23
dP1–M4	9	9.11 ± 0.27 (8.79–9.53) 2.95	6	8.92 ± 0.24 (8.48–9.19) 2.64	7	8.60 ± 0.23 (8.28–8.99) 2.71
P3–M3	11	6.22 ± 0.09 (6.07–6.35) 1.37	6	6.19 ± 0.41 (5.69–6.83) 6.68	7	5.93 ± 0.17 (5.74–6.22) 2.81
P3–M4	11	6.65 ± 0.11 (6.43–6.81) 1.71	6	6.44 ± 0.30 (6.10–6.88) 4.63	7	6.28 ± 0.17 (6.07–6.48) 2.77
M1–M3	11	4.95 ± 0.09 (4.83–5.08) 1.86	6	4.93 ± 0.21 (4.67–5.28) 4.28	7	4.71 ± 0.14 (4.57–4.98) 2.97
M1–M4	11	5.43 ± 0.15 (5.23–5.66) 2.72	6	5.36 ± 0.22 (5.08–5.64) 4.06	7	5.16 ± 0.17 (4.98–5.44) 3.32
LM1	11	1.80 ± 0.05 (1.70–1.88) 2.63	6	1.63 ± 0.14 (1.45–1.83) 8.83*	7	1.68 ± 0.10 (1.57–1.85) 5.87
WM1	11	1.57 ± 0.06 (1.47–1.68) 3.91	6	1.54 ± 0.05 (1.47–1.63) 3.56	7	1.55 ± 0.04 (1.52–1.63) 2.50
LM3	11	1.51 ± 0.06 (1.40–1.60) 3.93	6	1.48 ± 0.07 (1.42–1.60) 4.68	7	1.47 ± 0.08 (1.35–1.57) 5.59
WM3	11	1.50 ± 0.08 (1.30–1.60) 5.59	6	1.45 ± 0.07 (1.40–1.55) 4.75	7	1.49 ± 0.04 (1.42–1.55) 2.76
dp2–m3	9	7.22 ± 0.15 (6.99–7.44) 2.12	6	7.23 ± 0.47 (6.73–8.05) 6.51	7	6.95 ± 0.21 (6.65–7.19) 3.01
dp2–m4	9	8.03 ± 0.22 (7.65–8.38) 2.71	6	7.79 ± 0.40 (7.16–8.36) 5.18	7	7.71 ± 0.26 (7.29–8.03) 3.43
m1–m3	10	5.29 ± 0.09 (5.13–5.41) 1.61	6	5.16 ± 0.21 (4.90–5.41) 4.11	7	5.07 ± 0.12 (4.88–5.23) 2.44
m1–m4	10	6.11 ± 0.14 (5.82–6.30) 2.26	6	6.10 ± 0.27 (5.79–6.40) 4.39	7	5.79 ± 0.20 (5.49–6.07) 3.46
p3–m3	10	6.06 ± 0.09 (5.87–6.17) 1.47	6	5.99 ± 0.30 (5.66–6.35) 4.94	7	5.77 ± 0.19 (5.49–5.99) 3.27
p3–m4	10	6.90 ± 0.14 (6.55–7.09) 2.06	6	6.86 ± 0.32 (6.53–7.19) 4.7	7	6.54 ± 0.26 (6.12–6.88) 3.99
Lm1	10	1.83 ± 0.05 (1.73–1.88) 2.49	6	1.83 ± 0.09 (1.73–1.96) 4.81	7	1.76 ± 0.06 (1.68–1.83) 3.61
Wm1	10	0.94 ± 0.07 (0.84–1.04) 7.88*	6	0.92 ± 0.05 (0.84–0.97) 5.91	7	0.91 ± 0.06 (0.84–0.99) 6.32

194422). The maxillary bone extends posterodorsally to where the zygomatic arch begins. The lachrymal bone presents a single lachrymal foramen, placed dorsal to the anterodorsal extension of the jugal bone, contained by a bony wall, not exposed or visible laterally. The infraorbital foramen is circular and large, clearly visible in lateral view. In only a few specimens (e.g., FMNH 174481) a small accessory foramen appears dorsally. The posterior edge of the infraorbital foramen is located generally dorsal to the medial part (ectoflexus) of M1, sometimes anteriorly (above stylar cusp B [StB]), in a few specimens over stylar cusp C+D (StC+D; e.g., USNM 194412), and in only 1 specimen (FMNH 169817) between P3 and M1. The zygomatic arch in *L. inca* decreases in height from the anterior portion of the jugal, narrowing near its posterior contact with the squamosal and without a strong ventral inflection (Fig. 3). The jugal portion of the zygomatic arch covers the large maxillary foramen (the foramen internally separating the lachrymal from the maxillary bones) inside the orbit. This foramen is bounded by the lachrymal dorsally, a small portion of the palatine posteriorly, and by the maxillary ventrally (e.g., USNM 194407). Two foramina (1 anterodorsal, the other posteroventral) can be seen in lateral view immediately below the ventral inflection of the zygomatic arch, both contained by the palatine bone. The anterodorsal foramen occurs between the palatine bone and the nasal cavity, whereas the posteroventral foramen is located at the external and posterior edge of the palatine ridge. The palatine ridge in *L. inca* is robust, as in other caenolestids. The ridge is somewhat straight with a slight anterior inflection, and shows 2 posterior openings: the buccal one is the above-mentioned posteroventral opening, and a 2nd anterodorsal foramen occurs between the palatal area and the basicranium.

As in all caenolestids, the palate of *L. inca* is strongly fenestrated, with large to very large maxillopalatine fenestrae,

Table 3.—One-way analysis of variance between males and females of *Lestoros inca* by locality, using all external and craniodental measurements. Asterisks denote significant differences (if any) at Bonferroni-corrected *P*-values of 0.01 (*) and 0.02 (**) for external measurements, and 0.0015625 (*) and 0.0003125 (**) for craniodental measurements, following Rice (1989) and Cerqueira and Lemos (2000). Variables are defined in the text.

	Cedrobamba			Pillahuata			Torontoy			La Esperanza			Limacpunco		
Variable	*F*	*d.f.*	*P*-value	*F*	*d.f.*	*P*-value	*F*	*d.f.*	*P*-value	*F*	*d.f.*	*P*-value	*F*	*d.f.*	*P*-value
TTL	4.274219	16	0.055266	0.13247	22	0.71936	3.3253	18	0.084872	30.28011	42	0.000002* **	11.56341	11	0.005924* **
HBL	3.233607	16	0.091035	0.287286	22	0.597343	0.89774	19	0.355284	10.8843	42	0.001982*	3.24542	11	0.099067
TL	0.80822	16	0.381978	0.075838	23	0.785478	1.5626	18	0.227293	15.78126	42	0.000274* **	24.10827	11	0.000464* **
E	1.036429	16	0.323802	0.220055	23	0.643414	0.8717	19	0.362199	5.22009	42	0.027444	13.02285	11	0.004107*
F	2.422613	16	0.139152	1.464676	23	0.238479	17.04261	19	0.000572* **	15.05054	42	0.000363* **	3.95388	11	0.07222
GSL	4.064101	10	0.07146	0.104662	5	0.759398	3.66187	13	0.077947	0.43851	5	0.537137	5.67917	8	0.044331
ZB	6.17003	12	0.028749	0.078686	5	0.790322	2.24275	14	0.156446	4.19904	5	0.095746	1.9257	8	0.202657
PL	3.892933	10	0.076754	0.792759	5	0.414052	2.8303	15	0.113195	0.00276	5	0.960113	3.24938	8	0.109118
CW	5.214231	14	0.038538	0.459461	5	0.527968	7.0167	18	0.016327	0.60418	5	0.472143	0.40265	8	0.54344
PWP3	2.122973	15	0.16572	0.076533	5	0.793124	0.71505	18	0.408873	0.41332	5	0.548607	1.05553	8	0.334295
PWM1	1.320023	15	0.268579	0.444685	5	0.534403	1.99312	18	0.175069	0.2038	5	0.670575	1.09249	8	0.32647
PWM3	0.038821	15	0.846448	1.936245	5	0.222811	8.26345	18	0.010083	1.89491	5	0.227097	1.70396	8	0.22806
LINOR	0.005469	16	0.941967	0.03747	5	0.85413	0.89345	18	0.357059	0.11157	5	0.751922	0.30652	8	0.594957
NSL	5.900663	15	0.028172	0.0057	4	0.943442	3.37977	18	0.082561	4.76035	4	0.094552	4.11321	8	0.077084
BW	0.945987	16	0.345219	0.255368	5	0.634802	1.27315	16	0.275812	0.62228	5	0.465942	5.43704	8	0.048031
CBL	3.805286	10	0.079654	0.206207	5	0.668788	2.17346	14	0.162539	0.10956	5	0.754064	4.71896	8	0.061596
BB	0.412321	16	0.529887	1.246547	5	0.314974	0.00466	16	0.946395	0.01455	5	0.908695	0.00467	8	0.947212
MW	1.466202	16	0.243529	0.744751	5	0.427589	0.38366	17	0.543865	1.37195	5	0.294253	5.59117	7	0.050004
MHp3	0.945131	15	0.346379	0.869296	5	0.393947	1.80286	17	0.197022	1.01711	5	0.35949	6.26163	7	0.040853
MHm3	1.398905	16	0.254185	0.558622	5	0.488454	1.62629	17	0.21937	0.0212	5	0.889927	2.52426	9	0.14657
dP1–M3	0.507533	15	0.487143	0.579356	5	0.480902	5.24355	17	0.035088	0.0473	5	0.836425	1.70226	9	0.224365
dP1–M4	0.454553	16	0.509805	0.020323	5	0.892205	3.39676	17	0.082832	0.08435	5	0.783142	0.50724	9	0.494385
P3–M3	0.160282	15	0.694541	0.497747	5	0.511994	4.27302	17	0.054298	0.04736	5	0.836329	1.08886	9	0.323941
P3–M4	1.056198	16	0.319371	1.999114	5	0.216524	2.28199	17	0.149248	0.78874	5	0.415156	0.31019	9	0.591143
M1–M3	0.22431	16	0.642173	0.000064	5	0.993919	0.29379	17	0.594836	0.03807	5	0.852989	1.72032	9	0.222123
M1–M4	0.841916	16	0.372474	0.007645	5	0.933718	0.13242	17	0.720427	0.72862	5	0.432311	0.04366	9	0.839132
LM1	1.092996	16	0.311347	0.176502	5	0.69184	2.6454	17	0.122242	1.0934	5	0.343612	0.07031	9	0.796865
WM1	3.774996	16	0.069834	0.035128	5	0.858695	0.84676	17	0.370345	5.52743	5	0.065475	0.29304	8	0.603021
LM3	0.409924	16	0.531071	0.050959	5	0.830341	0.1149	17	0.738782	0.2515	5	0.637316	1.88319	8	0.207214
WM3	0.209274	16	0.653488	1.755429	5	0.242514	0	17	0.999736	0.59892	5	0.473975	5.99567	8	0.040024
dp2–m3	1.111808	16	0.307353	0.208534	5	0.667072	0.77013	16	0.393165	0.01657	4	0.903799	4.46854	7	0.072371
dp2–m4	0.394949	16	0.538578	0.910132	5	0.383891	1.29972	16	0.271043	0.08741	4	0.78221	0.76394	7	0.411079
m1–m3	0.194633	16	0.664992	2.466683	5	0.177082	1.79131	17	0.198393	0.13609	5	0.727303	0.05814	8	0.81553
m1–m4	0.007195	16	0.933453	1.975315	5	0.218872	2.33645	17	0.14477	0.02911	5	0.87122	0.07798	8	0.787133
p3–m3	0.119345	16	0.734246	0.703797	5	0.439764	3.02882	17	0.099866	0.00448	5	0.949248	0.02869	8	0.869699
p3–m4	0.566801	16	0.462467	1.63652	5	0.256952	2.63727	17	0.122778	0.11709	5	0.746127	0.01401	8	0.908697
Lm1	0.006253	16	0.937955	0.127818	5	0.735301	1.24095	17	0.28079	3.57126	5	0.117394	0.41275	8	0.53855
Wm1	0.493374	16	0.492519	0.049855	5	0.832151	0.016	17	0.900812	0.00545	5	0.944023	5.86382	8	0.04175

Table 4.—One-way analysis of variance between males and females of *Lestoros inca* grouped by localities using all external and craniodental measurements. Asterisks denote significant differences (if any) at Bonferroni corrected *P*-values of 0.01 (*) and 0.02 (**) for external measurements, and 0.0015625 (*) and 0.0003125 (**) for craniodental measurements, following Rice (1989) and Cerqueira and Lemos (2000). Oco-Cedro-Toron: Ocobamba, Cedrobamba, Torontoy; Espe-Pilla: La Esperanza, Pillahuata. Variables are defined in the text.

	Oco-Cedro-Toron			Espe-Pilla		
Variable	*F*	*d.f.*	*P*-value	*F*	*d.f.*	*P*-value
TTL	6.07192	42	0.017911	12.50711	66	0.000747* **
HBL	3.82593	43	0.056982	7.16158	66	0.009384*
TL	2.40539	42	0.128421	5.55237	67	0.021388
E	3.49483	43	0.06838	4.36196	67	0.040553
F	14.07237	43	0.000522* **	12.90085	67	0.000621* **
GSL	5.47049	28	0.026705	0.6102	12	0.449851
ZB	5.32425	32	0.027651	1.09868	12	0.315208
PL	4.90523	31	0.034257	0.72408	12	0.411466
CW	9.23089	40	0.004179	0.71521	12	0.414265
PWP3	1.54792	41	0.220508	0.47089	12	0.505622
PWM1	4.16595	41	0.047717	0.4732	12	0.504599
PWM3	5.34891	41	0.02583	0.1924	12	0.66872
LINOR	0.09646	42	0.757658	0.04149	12	0.842009
NSL	9.43432	41	0.003773	1.68521	10	0.223374
BW	3.70653	38	0.061709	0.51261	12	0.487712
CBL	3.97966	29	0.055526	0.38366	12	0.547233
BB	0.03688	38	0.848735	0.99402	12	0.338443
MW	1.21297	41	0.277168	0.28625	12	0.602409
MHp3	4.07543	40	0.05025	0.00755	12	0.932179
MHm3	3.162	41	0.082787	0.15414	12	0.70149
dP1–M3	6.8499	40	0.012452	0.27729	12	0.60808
dP1–M4	4.64097	41	0.037145	0.0235	12	0.880717
P3–M3	3.76667	40	0.059354	0.38566	12	0.546205
P3–M4	3.44715	41	0.070556	2.8266	12	0.118535
M1–M3	0.01088	41	0.917437	0.17817	12	0.680414
M1–M4	0.49856	41	0.484126	0.28132	12	0.605513
LM1	1.96262	41	0.168758	0.1628	12	0.693691
WM1	1.554	41	0.219622	1.32957	12	0.271334
LM3	0.33403	41	0.566459	0.38101	12	0.548595
WM3	0.35806	41	0.55288	0.39884	12	0.539532
dp2–m3	0.96988	40	0.33063	0.22351	11	0.645622
dp2–m4	3.66563	40	0.062717	0.23728	11	0.635741
m1–m3	2.17805	41	0.147631	0.56876	12	0.465294
m1–m4	1.88819	41	0.176872	0.96561	12	0.345176
p3–m3	2.9677	41	0.092479	0.31299	12	0.58614
p3–m4	2.77748	41	0.103221	1.22736	12	0.289633
Lm1	0.48074	41	0.491996	0.90481	12	0.360263
Wm1	0.07219	41	0.789526	0.00686	12	0.93536

and long and broad incisive fenestrae. Incisive fenestrae are commalike, with the broadest openings toward their posterior ends. They extend from the anterior border of I3 or the contact between I2 and I3 to the anterior of dP2, in some specimens (e.g., FMNH 172044) slightly posterior to this point. Maxillopalatine fenestrae extend from the anterior border of P3 to the posterior of M4 or almost to the base of the palatal ridge. In general, these fenestrae appear slightly wider anteriorly than posteriorly, although in some specimens (e.g., USNM 194421) they are equally wide. A bony separation between maxillopalatine fenestrae that is formed by a portion of the maxillary and palatine bones is present in a few samples (e.g., USNM 194389, USNM 194391, and USNM 194420). Some specimens (e.g., USNM 194426) have bony projections from the palatine toward the middle of these fenestrae, or from the external contact between maxillary and palatine bones toward the middle of the fenestrae (e.g., USNM 194430, USNM 194431, and FMNH 172050). At the posterior end of the palate, the palatine ridge is robust in all caenolestids and *L. inca* is no exception. The anterior portion of the zygomatic arch is not abruptly widened or projecting sideways, expands swiftly as a projection anterior to M3, and makes the orbit appear smaller than in other caenolestids. The glenoid fossa is limited by a robust postglenoid process that projects exteriorly from the skull and also forms a small posterior shelf, with the portion of the squamosal bone at a different level. In other words, there is a well-marked sulcus between the postglenoid process and the tympanic bulla at the alisphenoid base. The longest axis of the glenoid fossa follows the anteroposterior axis of the crania. The tympanic bulla in *L. inca* is intermediate in size between that of *Caenolestes* spp. and *R. raphanurus*, especially in its alisphenoid portion.

Table 5.—One-way analysis of variance between specimens assigned to *Lestoros inca* and *Caenolestes gracilis* using all external and craniodental measurements. Asterisks denote significant differences (if any) at Bonferroni corrected *P*-values of 0.01 (*) and 0.02 (**) for external measurements, and 0.0015625 (*) and 0.0003125 (**) for craniodental measurements, following Rice (1989) and Cerqueira and Lemos (2000). Variables are defined in the text.

Variable	*F*	*d.f.*	*P*-value
TTL	1.19556	127	0.27628
HBL	0.00089	128	0.976311
TL	3.20495	128	0.07578
E	1.64603	129	0.201801
F	5.15319	129	0.024862
GSL	0.0011	53	0.973672
ZB	1.803	58	0.184582
PL	0.00358	56	0.952499
CW	0.71618	66	0.400457
PWP3	0.02518	67	0.874389
PWM1	0.00981	67	0.921395
PWM3	0.04867	66	0.826067
LINOR	1.14363	67	0.288723
NSL	0.01159	65	0.914587
BW	1.56257	63	0.215913
CBL	0.02054	54	0.88658
BB	10.04566	64	0.002343
MW	0.10978	67	0.741427
MHp3	0.2317	66	0.631856
MHm3	3.71374	69	0.058085
dP1–M3	0.6555	68	0.420976
dP1–M4	1.51427	69	0.222667
P3–M3	0.16634	68	0.684668
P3–M4	0.40304	69	0.527622
M1–M3	5.76773	69	0.019021
M1–M4	0.23075	69	0.632487
LM1	0.16023	69	0.690182
WM1	0.00997	68	0.920771
LM3	1.52917	68	0.220491
WM3	1.09744	68	0.298538
dp2–m3	2.32608	65	0.132073
dp2–m4	1.40108	65	0.240854
m1–m3	0.90998	68	0.343498
m1–m4	0.8363	68	0.363688
p3–m3	0.59987	68	0.441313
p3–m4	1.64794	68	0.203597
Lm1	2.53089	68	0.116276
Wm1	0.82732	68	0.366261

The foramen magnum in *L. inca* is large and circular in shape. In lateral and ventral view the basioccipital bone is curved and the atlas bone of the vertebral column articulates more ventrally than in the other 2 genera.

In a general view (i.e., dorsal, lateral, and ventral), the crania of *L. inca* resembles that of *Caenolestes* spp. both in size and shape, and it is clearly different from that of *R. raphanurus*, which has an elongated rostrum or snout (Fig. 3). The zygomatic arch in *L. inca* is different from that found in *Caenolestes* spp. and *R. raphanurus*, decreasing in height from the anterior portion of the jugal, narrowing near its posterior contact with the squamosal, and without a strong ventral inflection (Fig. 3). This dorsoventral development conceals the large maxillary foramen (the one internally separating the lachrymal from the maxillary bones), which is easily observed above the jugal in *Caenolestes* spp. Slightly inflated nasals, dorsal to the antorbital vacuity (Osgood 1921), also differentiate *L. inca* from the other 2 genera (Fig. 3). In ventral view, the crania of *L. inca* and *Caenolestes* spp. are very similar as well, and they are clearly different from that of *R. raphanurus*. As in all caenolestids, the palate is strongly fenestrated, with large to very large maxillopalatine fenestrae, and long and broad incisive fenestrae, which appear different than those of *R. raphanurus* but similar to those of *Caenolestes* spp. (Table 9). The anterior portion of the zygomatic arch is not abruptly widened or projecting sideways as in *Caenolestes* spp. and *R. raphanurus*, where the arch is clearly expanded perpendicularly from the maxillary bone. This makes the orbit appear

Table 6.—Variable contributions and eigenvalues of the first 2 axes in a principal component (PC) analysis of external measurements from *Lestoros inca*. Variables are defined in the text.

Variable	PC1	PC2
TTL	0.53	0.06
HBL	0.65	−0.65
TL	0.43	0.68
E	0.24	0.23
F	0.21	0.24
Eigenvalue	0.0017	0.00068
% explained variance	56	23

Table 7.—Variable contributions and eigenvalues of the first 2 axes in a principal component (PC) analysis of craniodental measurements from *Lestoros inca*. Variables are defined in the text.

Variable	PC1	PC2
GSL	0.12	−0.25
ZB	0.07	−0.31
PL	0.19	−0.29
PWP3	0.11	−0.26
PWM1	0.1	−0.23
PWM3	0.06	−0.14
NSL	0.23	−0.3
BW	0.05	−0.2
CBL	0.16	−0.3
BB	−0.02	−0.2
dP1–M3	0.17	−0.12
dP1–M4	0.18	−0.09
P3–M3	0.24	0.07
P3–M4	0.26	0.12
M1–M3	0.21	0.19
M1–M4	0.22	0.21
LM1	0.34	0.35
WM1	0.13	0.01
LM3	0.12	0.28
WM3	0.19	0.01
dp2–m3	0.22	−0.08
dp2–m4	0.21	−0.01
m1–m3	0.21	0.02
m1–m4	0.20	0.07
p3–m3	0.24	0.04
p3–m4	0.23	0.09
Lm1	0.21	0.1
Wm1	0.20	−0.07
Eigenvalue	0.01	0.0015
% explained variance	55	15

TABLE 8.—Variable contributions and eigenvalues of the first 2 axes in a principal component (PC) analysis of dental measurements from *Lestoros inca*. Variables are defined in the text.

Variable	PC1	PC2
dP1–M3	0.16	0.1
dP1–M4	0.18	0.04
P3–M3	0.26	0.02
P3–M4	0.29	−0.03
M1–M3	0.24	−0.08
M1–M4	0.27	−0.1
LM1	0.39	−0.00022
WM1	0.14	0.13
LM3	0.14	−0.21
WM3	0.14	−0.18
dp2–m3	0.23	−0.01
dp2–m4	0.23	−0.11
m1–m3	0.23	−0.05
m1–m4	0.24	−0.1
p3–m3	0.28	−0.15
p3–m4	0.26	−0.12
Lm1	0.23	0.05
Wm1	0.21	0.9
Eigenvalue	0.01	0.00064
% explained variance	67	8

larger than in *L. inca*, which might be related to a larger eye in *Caenolestes* spp. and *R. raphanurus*. The area posterior to the postglenoid process (and anterior to the tympanic bulla) forms a small shelf in which a portion of the squamosal bone appears more ventrally located, a pattern not observed in *Caenolestes* spp. The foramen magnum in *L. inca* is more ventrally oriented than in *Caenolestes* spp., which probably implies that the head carriage in *L. inca* is slightly more vertical, thus allowing a wider range of movements than in *Caenolestes* spp.

Mandibles.—Mandibles appear short and robust in *L. inca*, with a broad masseteric fossa (Fig. 4). The coronoid crest forms an angle close to 90°, and the tip of the coronoid is close to the tip of the mandibular condyle (Fig. 4). Mandibles of *Caenolestes* spp. and *R. raphanurus* are slender, have smaller masseteric fossae, and the coronoid crest forms an obtuse angle (>90°; Table 9).

Dentition

Incisors.—The 1st incisors are slightly proodont in lateral view. In ventral view, they are clearly separated at the alveolus and in contact at their tip. The 1st and 2nd upper incisors (I1 and I2) show some lingual wear (e.g., USNM 194426), probably as a consequence of the contact between them and the procumbent lower incisors. I2 and I3 are similar in shape but I3 is slightly smaller. I4 is clearly different in crown shape from I2 and I3, and is separated from I3 by a diastema (Fig. 3). The shape of I4 is different from that of the preceding ones, is less compressed laterally, and is shorter anteroposteriorly.

The 1st lower incisor is procumbent, shovel-like, and in specimens with very little wear (e.g., FMNH 172048) shows a lateral (labial) cutting edge from where the tooth leaves the alveolus to its tip. Differences in length were found between

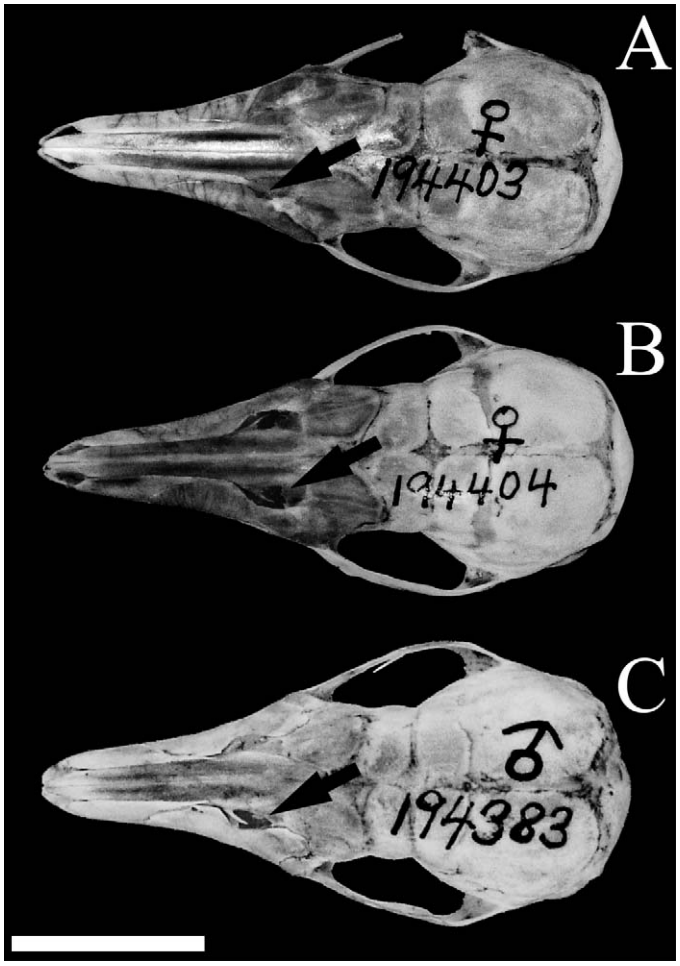

FIG. 2.—Dorsal view of the crania of *Lestoros inca* showing variation in the antorbital vacuity, from almost fully ossified in specimen A) USNM 194403, to opened and unossified in specimens B) USNM 194404 and C) USNM 194383. White scale bar: 1 cm. See text for discussion.

young specimens (with little or no molar wear) and older ones (e.g., USNM 194413 and USNM 194422), incisors in older specimens being two-fifths to one-fourth longer than those of younger ones; showing a continuous dental and mandibular growth until individuals reach adult size or the teeth are fully erupted. The procumbent incisor, apparently homologous to i2 in other marsupials (Hershkovitz 1995), is followed by 4 incisor-like teeth. The crowns of these incisor-like teeth have a unique pattern: when they erupt from the alveoli they widen toward the tip in a transversal (i.e., labiolingual) axis, whereas the crown has a longitudinal hammerhead-like orientation. These teeth markedly decrease in crown size from the 1st to last, with the 1st being more than 2 times longer in crown size and at almost twice as wide at root level as the last (Fig. 4). Along its posterior edge, each tooth has a groove where the hammerhead crown of the following tooth inserts. This groove is large in the 1st incisor-like tooth (i3?) and is smaller in each succeeding tooth, becoming almost obliterated in the last incisor-like tooth. This groove was observed in specimens with little wear (e.g., USNM 194417), in older specimens with

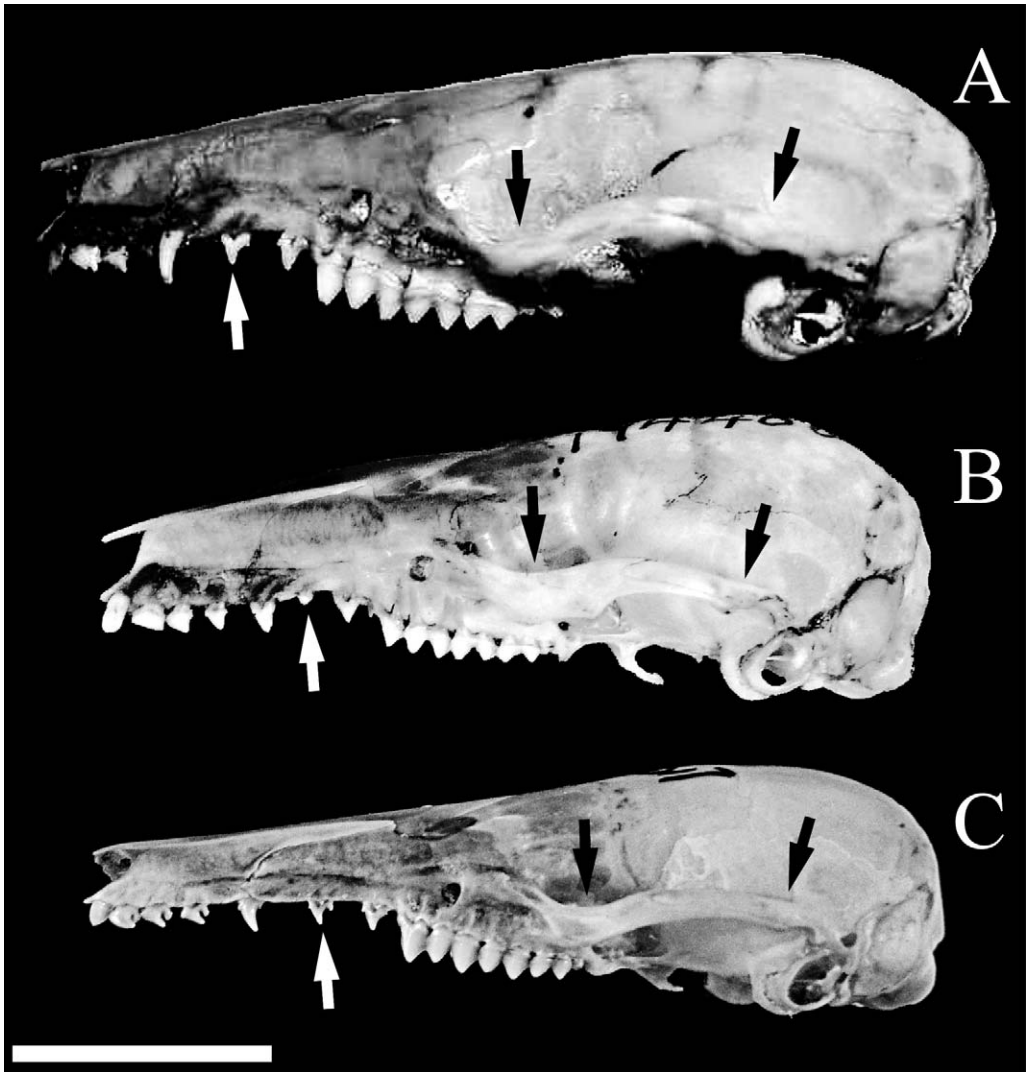

Fig. 3.—Lateral views of the crania of A) *Caenolestes caniventer*, B) *Lestoros inca*, and C) *Rhyncholestes raphanurus*. Black arrows indicate the anterior and posterior portions of the zygomatic arch (jugal and squamose bones, respectively), showing the broad anterior and narrow posterior of the zygomatic arch in B) *L. inca*, and the homogenous zygomatic arch breadth of A) *C. caniventer* and C) *R. raphanurus*. White arrows indicate size and shape differences in dP1, showing a peglike dP1 in B) *L. inca* and premolariform dP1 in A) *C. caniventer* and C) *R. raphanurus*. White scale bar: 1 cm. See text for discussion.

moderately worn teeth (e.g., USNM 194422), and even in specimens with heavily worn teeth (e.g., USNM 194413).

Canines.—The C1 in *L. inca* is double-rooted and premolariform in shape, with variation in crown shape. In some specimens there is an anterior cusp, others have a posterior cusp (and no anterior cusp), and some have both. This character (among a few others) was used by Bublitz (1987) to separate the forms *C. inca* from *C. gracilis*. In this study, accessory cusps were found in all populations, and in both males and females, giving no support to use of these cusps as a distinguishing character between forms or sexes. In general, the tooth is similar in size to dP2 but looks as if the crown orientation would be exactly the opposite, as if the tooth would be flipped 180°. Lower canines, if present (see above), are indistinguishable from the other incisor-like teeth anterior to dp2.

Premolars.—The dP1 is small and morphologically variable. Apparently "peglike" in some specimens (e.g., FMNH 172048), it looks like a small "typical" premolar in others (i.e., with a laterally compressed crown, a central cusp, and a small talon; e.g., FMNH 174481). Its small size and position behind C1 exposes this tooth to rapid wear, resulting in the loss of distinguishable crown relief. The dP1 of all analyzed specimens shows 2 roots; specimens that apparently have a single root (e.g., USNM 194417) show 2 fused roots with a central groove when seen through a stereoscope. This tooth may be absent from the toothrow in 1 of the sides (e.g., FMNH 75112, FMNH 75122, and FMNH 174485) or in both (e.g., FMNH 75120). The dP2 is similar in size to C1, with a sharp central cusp without associated crests, and is variable in general structure. Some specimens have a short talon (e.g., USNM 194425), others a very sharp central cusp without a

TABLE 9.—Compared craniodental characters diagnostic of *Lestoros inca*, *Caenolestes* spp., and *Rhyncholestes raphanurus*.

Character	*Lestoros inca*	*Caenolestes* spp.	*Rhyncholestes raphanurus*
Elongation of the rostrum	Moderate	Moderate	Well developed
Inflated nasals (dorsal to the antorbital vacuity)	Yes	No	No
General aspect of the zygomatic arch	Robust	Slender	Slender
Zygomatic arch width (Fig. 3)	Not homogenous, narrowing in its distal portion	Mostly homogenous	Mostly homogenous
Development of lambdoid crests	Poorly or not developed	Well developed	Variable (well developed to not developed)
Shape of incisive fenestrae	Commalike, broader at posterior end	Commalike, broader at posterior end	Somewhat straight and of constant width
Angle of the coronoid crest with the dentary (Fig. 4)	Almost straight (90°)	Obtuse angle (>90°)	Obtuse angle (>90°)
Crown shape on I3 and I4	I4 clearly different, premolariform in shape	I3 and I4 similar in crown shape	I3 and I4 similar in crown shape
Diastema between I3 and I4	Present	Absent	Absent
Size of i3 (Fig. 4)	Large	Small	Small
Posterior groove in incisor-like teeth (i3–4, c1, and dp1)	Present	Absent	Absent
C1 shape and root number	Double rooted and premolar-like	Single rooted and caninelike	Single rooted, caninelike or premolar-like
Size of dP1 (Fig. 3)	Very small in relation to dP2	Subequal to dP2	Subequal to dP2
dp2 longer than p3 in occlusal and labial view	Yes	Yes	No, dp2 < p3
Development of labial cingula in M1–3	Absent or not developed	Well developed	Moderately developed
Comparative size of m4 with trigonid of m3	Subequal to m3 trigonid	Longer than m3 trigonid	Shorter than m3 trigonid
Development of the anterobasal cingulum	Well developed	Poorly developed	Moderately developed
Height of the trigonid in relation to that of the talonid	Taller or well-marked difference between trigonid and talonid basins	Taller or well-marked difference between trigonid and talonid basins	Trigonid and talonid basins at the same height
Development of a labial cingulum between protoconid and entoconid	Well developed or marked	Poorly developed	Poorly developed

talon and anterior cingulum (e.g., USNM 194432), or the inverted morphology of C1, with an anterior cingulum (e.g., USNM 194435). The P3 is the tallest tooth in the maxilla; it has an anterior cusp variable in size (usually well developed and larger in males) and a strong and trenchant central cusp with an associated posterior crest. Although this tooth is obliquely oriented, its major crest is in line with the cutting edges of StB and StC+D on M1–3, which together form a trenchant, well-aligned cutting edge. This tooth also has a lingual cingulum, extending from the anterior cusp and toward the tooth's distal end, where it joins the posterior crest that comes from the main cusp (e.g., FMNH 174489).

Only dp2 and p3 are distinguishable among the lower antemolar teeth. The dp2 is longer than the p3 in lateral and occlusal view, with p3 being narrower in crown size than dp2 (especially at the talon) but taller in lateral view. The dp2 is "typical" in shape and similar to a didelphid premolar, with a well-developed central cusp and talon, and an anterior accessory cusp slightly displaced lingually, which becomes quickly worn. The p3 has a large central cusp, with a symmetric (equidistant) position, a more-developed talon that is higher on the labial side, and a developed posterior cusp in specimens with little or no wear.

Molars.—Upper molars decrease in size from M1 to M4, with M1 and M2 being subequal, M3 clearly smaller, and M4 very small, single-rooted, and peglike. All molars in lateral view show well-developed and subequal StB and StC+D (Fig. 1A). These cusps are larger on M1, slightly smaller on M2, and distinctly smaller on M3, following the size progression described above. M2 has the largest occlusal surface in *L. inca*. On M3, which has a more triangular shape, a reduction of the posterolingual area is evident. All upper molars have a well-developed lingual cingulum (light gray shading in Fig. 1A), between the inflection of the postprotocrista and the premetaconular crest (very obvious in USNM 194319, not so in specimens with heavily worn teeth). In lateral view, cusp heights on M1 and M2, from taller to lower, are as follows: StC+D → StB → protocone → metaconule. On M3, StB and protocone are equal in height. A small cusp anterolingual to StB (apparently the paracone) forms a small socket that increases in size from M1 to M3 (Fig. 1A). This structure is highly susceptible to wear and can only be observed in juveniles or specimens with very little wear. Associated with StC+D is the metacone, which appears slightly displaced anteriorly and increases in size from M1 to M3, just like the paracone (Fig. 1A). M4 is obliquely oriented and has a well-

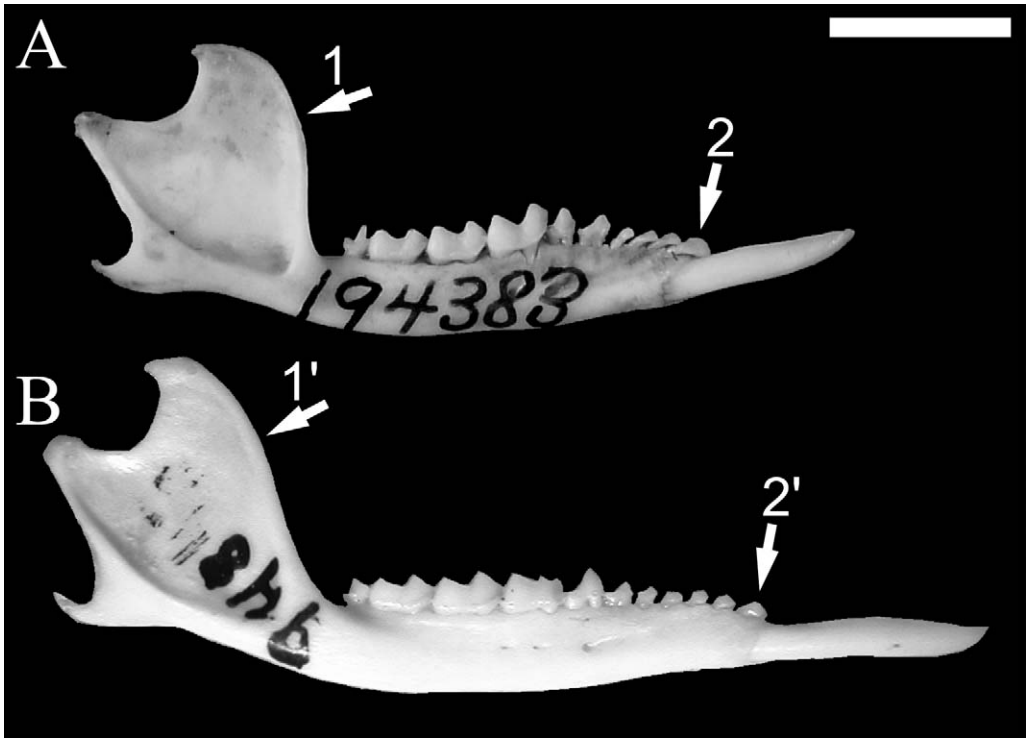

FIG. 4.—Mandibles of A) *Lestoros inca* and B) *Rhyncholestes raphanurus* in lateral view. Arrows 1 and 1′ show differences in the angle of the coronoid crest in *L. inca* (near 90°) and *R. raphanurus* (larger than 90°), respectively. Arrows 2 and 2′ show the marked size difference between i3 and the following incisor-like teeth in A) *L. inca* and similar-sized incisor-like teeth in B) *R. raphanurus*, respectively. White scale bar: 5 mm. See text for discussion.

developed medial crest that separates the anterolabial and posterolingual basins.

Lower molars in *L. inca* decrease in occlusal surface from m1, with m4 being subequal to m3's trigonid in length, and have a large, well-developed anterobasal cingulum. The 1st lower molar (m1) is the tallest tooth in lateral view, with the trigonid basin appearing taller than the talonid basin. The protoconid is the highest cusp, followed closely by an enormous entoconid and hypoconid (almost equal in height), the metaconid, and the paraconid. A well-developed preprotocristid is present on m2 and m3; the preprotocristid is slightly developed on m1. The paraconid is vestigial on m1 because it is associated with the paracristida and preprotocristida, which appear joined in a single crest. On m2 and m3 the paraconid is a more or less independent cusp; it is larger and more bulbous and is slightly displaced labially and behind the hypoconulid of the anterior tooth. Because of its position, the paraconid is probably not as susceptible to wear as on m1, but the paracristid is worn. The hypoconulid is progressively displaced posteriorly from m1 to m3. The entoconid is a well-developed crestiform structure, instead of a "typical" cusp. It varies in position from m1 to m3, being posterior to the hypoconid on m1, almost equal on m2, and anterior to this cusp on m3. *L. inca* has a tall and well-developed entocristid, which in some specimens (i.e., USNM 194395) encloses the talonid in its lingual side. The entocristid usually joins a crest that descends posteriorly from the metaconid, which is well developed on m2 and m3. Because these crests join, a well-developed lingual cingulum can be found between metaconid and entoconid (light gray shading in Fig. 1B). A notch that opens lingually can be found between hypoconulid and entoconid (dark gray shading in Fig. 1B).

Several differences were found between the dentition of *L. inca* and that of the other living caenolestids. Upper incisors in *L. inca* follow the size reduction observed in *Caenolestes* spp., but I4 is clearly different in crown shape from I2 and I3 (i.e., less compressed laterally and shorter anteroposteriorly) and is separated from I3 by a diastema (Fig. 3). In the lower dentition, size differences between the 1st incisor-like tooth and the other incisor-like teeth is unique to *Lestoros*. In both *Caenolestes* spp. and *Rhyncholestes* these teeth are similar in size, or slightly different, and the 1st incisor-like tooth is not larger than the rest (Fig. 4, arrows 2 and 2′). All incisor-like teeth of *L. inca* presented a posterior groove, a character not present in specimens of *Caenolestes* spp. and *R. raphanurus* analyzed. Upper canines are double-rooted in *L. inca*, a character unique to this species (Table 9). Some variation was documented in the presence of anterior or posterior cusps, or both, in the C1 of *L. inca*; this variation also was recorded in *R. raphanurus* but not in *Caenolestes* spp. The first 2 upper premolars in *L. inca* are different in size (dP1 is smaller than dP2) but these teeth are subequal in *Caenolestes* spp. and *R. raphanurus*. Despite P3 being the tallest tooth in all living caenolestids, size differences between this tooth and dP2 are evident in *Caenolestes* spp. and

Table 10.—Type, number, and sex of specimens with dental anomalies recorded for *Lestoros inca* for all individuals examined and separated by locality (only those with anomalous individuals). Anomaly types follow Martin (2007), i = indeterminate sex. See Appendix I for localities.

Type of anomaly	All specimens, $n = 70$ (28♀, 41♂, 1i)	Cedrobamba, $n = 17$ (6♀, 11♂)	Torontoy, $n = 21$ (10♀, 10♂, 1i)	La Esperanza, $n = 7$ (3♀, 4♂)	Pillahuata, $n = 7$ (2♀, 5♂)	Limacpunco, $n = 10$ (4♀, 6♂)
Supernumerary teeth	2 (2♂), 2.9%	1 (1♂)			1 (1♂)	
Missing teeth	14 (10♀, 4♂), 20%	1 (1♀)	5 (4♀, 1♂)	2 (1♀, 1♂)		6 (4♀, 2♂)
Fused teeth	3 (1♀, 1♂, 1i), 4.3%		1 (1i)	1 (1♀)		1 (1♂)
Anomalous shape	1 (1♀), 1.4%					1 (1♀)
Teeth in unusual position	1 (1♂), 1.4%				1 (1♂)	
Total no. specimens analyzed and % with anomalies	21 (12♀, 8♂, 1i), 30%	2 (1♀, 1♂), 11.8%	6 (4♀, 1♂, 1i), 28.6%	3 (2♀, 1♂), 42.9%	2 (2♂), 28.6%	8 (5♀, 3♂), 80%

R. raphanurus but not in *L. inca* (Fig. 3). In lower premolars, the pattern of occlusal size and lateral height of dp2 and p3 in *L. inca* is similar to that found *Caenolestes* spp., but different than in *R. raphanurus*, where dp2 is smaller than p3. In *Caenolestes* spp. (e.g., FMNH 53288), dp2 and p3 have a higher central cusp that is anteriorly displaced and the talon is broader and longer than in *L. inca*. The first 3 upper molars in *L. inca* lack a well-developed labial cingulum, which is present in *Caenolestes* spp. and is moderately developed in *R. raphanurus* (Table 9). Lower molars decrease in occlusal surface in all living caenolestids, but the magnitude of the size difference for m4 is distinct for each species. In general, m4 is shorter in *L. inca*, with a narrower trigonid and a less-developed talonid, and slightly rounded in comparison with *Caenolestes* spp., where m4 appears longer and less rounded. In most *Caenolestes* spp. m4 is clearly longer than the m3 trigonid; this tooth is distinctively smaller in *R. raphanurus* (Table 9). Lower molars in *L. inca* have a well-developed anterobasal cingulum (Fig. 1B), notably larger than in *Caenolestes* spp., despite the molars being slightly smaller in the former (Table 9). The trigonid basin appears taller than the talonid basin in *L. inca*, more so than in *Caenolestes* spp., a feature that clearly separates these genera from *R. raphanurus*, in which trigonid and talonid appear to be at the same height in lateral view (Table 9). The hypoconulid is progressively displaced posteriorly from m1 to m3, a pattern that is less marked in *Caenolestes* spp., where it appears more or less at the same distance (i.e., not displaced posteriorly from m1 to m3). The lingual cingulum formed between metaconid and entoconid also is present in *Caenolestes* spp. and *R. raphanurus*, but less developed than in *L. inca*.

Eruption sequence.—The youngest specimen examined is FMNH 172048, which is followed by FMNH 75113 and FMNH 75119. In each of these specimens, while M4 is still encrypted or its crown barely showing above the alveolus, P3 is not fully erupted and the main cusp is still lower than the following molar's StB in lateral view. In specimen FMNH 75113 this cusp is at the same level of StB or slightly higher, and in FMNH 75119 it is higher than all following molar cusps. Therefore, the following eruption sequence is given for *L. inca*: P3 → m4 → p3 → M4. This sequence also is corroborated by specimen FMNH 172048, in which P3 and m4 are in their final position, but m4 is slightly oriented transversely to the dental axis due to the mandible not being fully grown; p3 is still not in its place and M4 is partially encrypted. In this specimen, C1 is still erupting (i.e., not in its final position) and is slightly taller than dP2. In adult specimens with fully erupted teeth C1 is clearly taller than dP2 (e.g., FMNH 75115). Apart from this, the diastema between I3 and I4 is small, extending anteroposteriorly in FMNH 75113. The lower dentition shows the following pattern: procumbent incisor with little development beyond the alveolus (i.e., not fully erupted as in adult specimens), incisor-like teeth (most antemolars) without separation (i.e., crowded), and p3 with completely erupted crown but lower in height than dp2 and m1. In FMNH 75113 p3 is taller than any other premolar, but it has not acquired its final position (a similar pattern was observed in FMNH 75119). In specimen FMNH 75115 both p3 and the protocone of m1 are at the same height in lateral view. In specimen FMNH 172048, although m4 is erupted, it is not in its final position, that is, the hypoconulid of m3 is not placed between the anterior cingulum and paraconid, it is not in line with m1–3 and is still on the ascending mandibular ramus. The next specimen in this sequence of tooth development (FMNH 75113) has its hypoconulid already placed between paraconid and anterior cingulum of m4. All these observations are in agreement with those made for *Caenolestes* spp. and *R. raphanurus* by Luckett and Hong (2000) and can now be described as the general eruption pattern for the Caenolestidae.

Dental anomalies.—Among the specimens with complete skulls ($n = 70$), the percentage of anomalies in *L. inca* is 30% ($n = 21$; Table 10). Of all types of anomalies, missing teeth is the most commonly recorded ($n = 14$, 20%), followed by fused teeth ($n = 3$, 4.3%). Three other types of anomalies were found: supernumerary teeth (extra incisor-like tooth, USNM 194406; and extra tooth in the palate, FMNH 172052), shape anomalies (single-rooted m4, FMNH 75122), and a tooth in unusual position (crown of an extra tooth between C1 and dP1, FMNH 172052). A specimen with fused c1–dp2 or dp1–2 (FMNH 194948) shows the whole toothrow displaced forward, probably in response to the fused teeth. The list of anomalies and their frequency according to sex and locality is presented

in Table 10. Localities with the highest number of anomalies are Limacpunco ($n = 8$) and Torontoy ($n = 6$), whereas Limacpunco and La Esperanza show the highest number of anomalies per locality (80% and 42.8%, respectively). The number of anomalies found in *L. inca* is between those registered for *Caenolestes fuliginosus* and *R. raphanurus* (Martin 2007); no information is available for other *Caenolestes* species. As with *R. raphanurus*, missing teeth are the most commonly registered anomalies, especially incisor-like teeth, although in *L. inca* this category also can include missing dP1.

Discussion

In comparison to other living caenolestids, *L. inca* appears morphologically closer to *Caenolestes* spp. than to *R. raphanurus*, a feature that might have led Bublitz (1987) to conclude that this species should be part of the genus *Caenolestes*. Contrary to this, when 19 selected craniodental characters are compared (Table 9), *L. inca* and *Caenolestes* spp. share only 3 characters, whereas *Caenolestes* spp. and *R. raphanurus* share at least 10. Differences between the information presented herein and the descriptions of Bublitz (1987) might be related to the larger number of specimens analyzed (i.e., $n = 75$ versus $n = 33$ by Bublitz [1987]) and wider range of localities (i.e., large series from La Esperanza and Limacpunco were not available during the study made by Bublitz).

Analysis of variance to test for sexual dimorphism, individually or with pooled localities, showed no significant differences, except for some external measurements (Tables 3 and 4). This trend has been documented for some other South American marsupials (e.g., *Dromiciops gliroides*, *Lestodelphys halli*, and *Thylamys pallidior*—Martin 2005, 2008).

In this study, and as stated before by Myers and Patton (2007), extensive overlap was found between specimens assigned by Bublitz (1987) to the forms *C. inca* and *C. gracilis*. ANOVA performed to test the validity of *C. gracilis* as separate from *L. inca* showed no significant metric differences (Table 5). Also, when morphological characters used by Bublitz (1987) were analyzed, the intraspecific variation observed provided no means to differentiate *C. gracilis* from typical specimens of *L. inca*. Particularly variable were the antorbital vacuity (preorbital groove as designated by Bublitz [1987]), presence of an anterior style on the upper canine, and number of roots on dP1, lending support to consider *L. inca* as a single species.

In an anatomical context, several morphological characters clearly differentiate *Lestoros* from the other 2 genera of living caenolestids (*Caenolestes* and *Rhyncholestes*; Table 9). The crania of *L. inca* seems to be more robust because of the less-elongated rostrum and broader zygomatic arches. These features, combined with a shorter mandible with a deeper masseteric fossae, might indicate that *L. inca* feeds on tougher items than do other caenolestid species (a probable exception could be *Caenolestes condorensis*, which is much larger [Albuja and Patterson 1996]). Dental characters appear to show the most conspicuous differences between living caenolestid species (Table 9). In the upper dentition, the distinct morphology of I4 and its separation from other incisors, the double-rooted canine, and smaller dP1 might indicate differences in feeding preferences of *L. inca* from other caenolestids, which are still poorly known (Myers and Patton 2007). The posterior groove observed in all lower incisor-like teeth is a rare feature apparently unique to *L. inca*. Although its biological significance is unknown, it can be hypothesized that this groove would serve as a guide to the following tooth, which would erupt and grow (at least in the early stages) after this groove. In this way, the eruption pattern would start off with the procumbent incisor (I_2 of Hershkovitz [1995]) and be followed by incisor-like teeth 1, 2, 3, and 4 (here referred to i3, i4, c1, and dp1, respectively) very close to each other; when the mandible grows these teeth would start separating from each other. In all living caenolestids, the general pattern in the first 3 lower molars is the same: m1 with the trigonid narrower than the talonid (hypoconid is labially displaced and the cristida obliqua is very long); m2 has a narrower talonid than m1, but still wider than the trigonid; and m3 has a more quadrangular shape, with the trigonid and talonid equally wide. These differences can be attributed to modifications in 2 "areas." One is the pattern shown in the trigonid by the protoconid, which becomes more labially displaced from m1 to m3; the 2nd involves the hypoconid, which is labially displaced on m1 and seems to be lingually compressed on m3, making for a narrower talonid area. This implies that the trigonid is becoming wider and the talonid narrower with respect to the anterior tooth, and is correlated to the reduction in protocone and upper molar size from M1 to M3. The trigonid becomes progressively shorter from m1 to m3, due to an anterior displacement of the metaconid progressing from m1 (on which it is clearly posterior to the protoconid) to m3 (where it is in line with the protoconid). The size reduction in trigonid area and anterior displacement of the metaconid from m1 to m3 can be related to the occlusal relationships between lower and upper molars: there is a lingual shearing between the trigonid of m1 and the enlarged P3, whereas in m2 and m3 the talonid has a more prevalent crushing function, occluding with the protocones of the upper molars (M1–3).

The bladelike pattern and long shearing structures described herein for molars and premolars of *L. inca* (as well as in other caenolestids) are consistent with a diet of soft-bodied invertebrates, as proposed by Strait (1993). In this context, long crests such as those formed by the continuation of StB and StC+D, much taller than other molar cusps, would have a cutting function, with a crushing action performed by the other structures present in caenolestid teeth (i.e., protocone–talonid basin and trigonid–hypocone or metaconule). The posterior crest of P3 also contributes to these shearing structures, whereas the central cusps of C1, dP2, and P3 would help secure or puncture prey, or both. These patterns agree with reports on the diet of *Caenolestes* spp. and *R. raphanurus* (Patterson 2007 [2008]; Timm and Patterson 2007 [2008]; and

literature cited therein) and could be applied tentatively to *L. inca*.

Observations on the eruption pattern of *L. inca* conform to those made for *Caenolestes* spp. and *R. raphanurus* by Luckett and Hong (2000), confirming the general eruption pattern for the Caenolestidae. This pattern (P3 → m4 → p3 → M4) is different from those observed in other South American marsupials in which M4/m4 precedes P3/p3 (in both upper and lower dentitions, as in *Marmosops incanus*, *Lestodelphys halli*, *Monodelphis domestica*, and *Caluromys* spp.), or P3/p3 precedes M4/m4 (in both upper and lower dentitions, as in *Didelphis* spp. [Tribe 1990; Vidigal and Patton 1996; Martin 2005; van Nievelt and Smith 2005; Astúa and Leiner 2008]). Reasons for this eruption sequence, especially for P3, might be related to the functional importance (or lack thereof) of each tooth in the dentition of living and extinct caenolestids (e.g., P3 being the tallest tooth in the maxilla and probably having an important function securing prey; see above), or with the accelerated development when a tooth follows a vestigial or nonerupting predecessor, as proposed by Luckett (1993).

Although *L. inca* has a shorter rostrum and less-elongated mandibles than *Caenolestes* spp. and *R. raphanurus*, missing or supernumerary teeth occur as in the other species, probably as a result of the same functional pressures (or lack thereof) or adaptations in these species (e.g., no occlusion between lower incisor-like teeth). Also, *L. inca* and *Caenolestes* spp. inhabit the same type of isolated environments, which would be influenced by similar evolutionary constraints (i.e., genetic isolation, inbreeding, and limited gene flow), leading to anomalies in the same areas of the toothrow. As has been stated before (Martin 2007), anatomical work should provide a better understanding of the mechanisms involved in these processes.

In addition to describing the craniodental anatomy of *L. inca*, this work adds at least 13 well-marked craniomandibular and dental differences between *Lestoros* and *Caenolestes* spp. The information presented herein supports the idea that *Lestoros* is a valid genus of Paucituberculata, clearly different from *Caenolestes* and *Rhyncholestes*. As seen in *R. raphanurus* (Martin 2008), *L. inca* shows no sexual dimorphism in craniodental anatomy. Also, the lack of clinal variation and of significant differences between populations adds support to consider *L. inca* as a single species. As with most living organisms, *L. inca* shows a mosaic of derived and plesiomorphic characters, although several craniodental features (e.g., less-elongated snout and more-triangular M3) show that *L. inca* is less derived compared to *Caenolestes* spp. and *R. raphanurus*. Further studies should add more information that could shed some light on the relationships of these unique and understudied taxa.

Resumen

Los cenoléstidos comprenden un grupo poco conocido de marsupiales sudamericanos, cuya distribución se encuentra restringida a los ambientes de páramo y subpáramo en la Cordillera de los Andes desde Colombia y el oeste de Venezuela hasta Bolivia (representados por los géneros *Caenolestes* y *Lestoros*), y el bosque valdiviano del sur de Chile–Argentina donde habita *Rhyncholestes raphanurus*. Una de estas especies, el ratón runcho andino *Lestoros inca*, habita el páramo y subpáramo desde el sur del Perú al extremo norte de Bolivia. A pesar de ser común en trampeos, es poco lo que se conoce de esta especie en cuanto a variabilidad intraespecífica, patrón de erupción y anomalías dentarias, y otros rasgos anatómicos. El objetivo de este trabajo es analizar la variabilidad intraespecífica de *L. inca*, incluyendo una descripción anatómica del cráneo y dentición, analizar la variación clinal, patrones de erupción y anomalías dentarias. La falta de variación clinal o diferencias poblacionales significativas, brindó soporte al tratamiento de *L. inca* como una única especie. El patrón de erupción dentario encontrado en la especie (P3 → m4 → p3 → M4) confirma esta secuencia como el patrón generalizado para los paucituberculata vivientes. La falta de dientes, entre los incisivos procumbentes y el segundo premolar inferior, fueron la anomalía dentaria más comúnmente encontrada (20% de los ejemplares analizados). Comparaciones con cenoléstidos vivientes permiten considerar a *L. inca* como especie válida y claramente diferente del resto. La información aquí presentada podrá ser usada en estudios anatómicos y paleontológicos sobre cenoléstidos en particular y marsupiales en general, aportando, además, información anatómica que permitirá realizar inferencias en fósiles.

Acknowledgments

E. Watkins and M. Simeon provided economic support during parts of this study. M. Tejedor, B. Patterson, and an anonymous reviewer provided insightful comments and suggestions that added clarity to the manuscript. A. Abello generously provided the figure used for dental nomenclature. Curators R. Voss (AMNH), P. Jenkins (BMNH), B. Patterson (FMNH), G. D'Elía (IEEUACH), D. Flores (MACN), and A. Gardner (USNM) allowed access to specimens under their care. L. Gordon (USNM) and J. Phelps (FMNH) went beyond their normal duties to assist me during my visits to the institutions in which they work. My visit to the AMNH was funded by a Collection Study Grant.

Literature Cited

Abello, M. A. 2007. Sistemática y bioestratigrafía de los Paucituberculata (Mammalia: Marsupialia) del Cenozoico de América del Sur. Ph.D. dissertation, Universidad Nacional de La Plata, La Plata, Argentina.

Albuja V., L., and B. D. Patterson. 1996. A new species of northern shrew-opossum (Paucituberculata: Caenolestidae) from the Cordillera del Cóndor, Ecuador. Journal of Mammalogy 77:41–53.

Anderson, S. 1997. Mammals of Bolivia; taxonomy and distribution. Bulletin of the American Museum of Natural History 231:2–652.

Astúa, D., and N. O. Leiner. 2008. Tooth eruption sequence and replacement pattern in woolly opossums, genus *Caluromys* (Didelphimorphia: Didelphidae). Journal of Mammalogy 89:244–251.

Bedian, A. G., and K. W. Mossholder. 2000. On the use of the coefficient of variation as a measure of diversity. Organizational Research Methods 3:285–297.

Brown, B. 2004. Atlas of New World marsupials. Fieldiana: Zoology (New Series) 102:1–308.

BUBLITZ, J. 1987. Untersuchungen zur Systematik der rezenten Caenolestidae Trouessart, 1898: unter Verwendung craniometrischer Methoden. Bonner Zoologische Monographien 23:1–96.

CATTELL, R. B. 1966. The scree test for the number of factors. Multivariate Behavioural Research 1:245–276.

CERQUEIRA, R., AND B. LEMOS. 2000. Morphometric differentiation between Neotropical black-eared opossums, *Didelphis marsupialis* and *D. aurita* (Didelphimorphia, Didelphidae). Mammalia 64:319–327.

DI RIENZO, J. A., F. CASANOVES, M. G. BALZARINI, L. GONZALEZ, M. TABLADA, AND C. W. ROBLEDO. 2010. InfoStat versión 2010. Grupo InfoStat, FCA, Universidad Nacional de Córdoba, Córdoba, Argentina.

GOIN, F. J., A. M. CANDELA, M. A. ABELLO, AND E. V. OLIVEIRA. 2009. Earliest South American paucituberculatans and their significance in the understanding of 'pseudodiprotodont' marsupial radiations. Zoological Journal of the Linnean Society 155:867–884.

GOIN, F. J., M. SÁNCHEZ-VILLAGRA, M. A. ABELLO, AND R. F. KAY. 2007. A new generalized paucituberculatan marsupial from the Oligocene of Bolivia and the origin of 'shrew-like' opossums. Palaeontology 50:1267–1276.

HERSHKOVITZ, P. 1995. The staggered marsupial third lower incisor: hallmark of cohort Didelphimorphia, and description of a new genus and species with staggered i3 from the Albian (Lower Cretaceous) of Texas. Bonner Zoologische Beiträge 45:153–169.

KIRSCH, J. A. W., AND P. F. WALLER. 1979. Notes on the trapping and behavior of the Caenolestidae (Marsupialia). Journal of Mammalogy 60:390–395.

LUCKETT, P. W. 1993. An ontogenetic assessment of dental homologies in therian mammals. Pp. 182–204 in Mammal phylogeny: Mesozoic differentiation, multituberculates, monotremes, early therians and marsupials (F. S. Szalay, M. J. Novacek, and M. C. McKenna, eds.). Springer-Verlag, New York.

LUCKETT, P. W., AND N. HONG. 2000. Ontogenetic evidence for dental homologies and premolar replacement in fossil and extant caenolestids (Marsupialia). Journal of Mammalian Evolution 7:109–127.

MARSHALL, L. G. 1980. Systematics of the South American marsupial family Caenolestidae. Fieldiana: Geology (New Series) 5:1–145.

MARTIN, G. M. 2005. Intraspecific variation in *Lestodelphys halli* (Marsupialia: Didelphimorphia). Journal of Mammalogy 86:793–802.

MARTIN, G. M. 2007. Dental anomalies in *Dromiciops gliroides* (Microbiotheria, Microbiotheriidae), *Caenolestes fuliginosus* and *Rhyncholestes raphanurus* (Paucituberculata, Caenolestidae). Revista Chilena de Historia Natural 80:393–406.

MARTIN, G. M. 2008. Sistemática, distribución y adaptaciones de los marsupiales Patagónicos. Ph.D. dissertation, Universidad Nacional de La Plata, La Plata, Argentina.

MYERS, P., AND J. L. PATTON. 2007 [2008]. Genus *Lestoros* Oehser, 1934. Pp. 124–126 in Mammals of South America, Volume 1: marsupials, xenarthrans, shrews, and bats (A. L. Gardner, ed.). University of Chicago Press, Chicago, Illinois.

OSGOOD, W. H. 1921. A monographic study of the American marsupial *Caenolestes*. Field Museum of Natural History, Zoological Series 16:1–162 + 22 plates.

PATTERSON, B. D. 2007 [2008]. Genus *Rhyncholestes* Osgood, 1924. Pp. 126–127 in Mammals of South America, Volume 1: marsupials, xenarthrans, shrews, and bats (A. L. Gardner, ed.).University of Chicago Press, Chicago, Illinois.

RICE, W. R. 1989. Analyzing tables of statistical tests. Evolution 43:223–225.

STRAIT, S. G. 1993. Molar morphology and food texture among small-bodied faunivorous mammals. Journal of Mammalogy 74:391–402.

THOMAS, O. 1917. Preliminary diagnoses of new mammals obtained by the Yale–National Geographic Society Peruvian Expedition. Smithsonian Miscellaneous Collections 68:1–3.

TIMM, R. M., AND B. D. PATTERSON. 2007 [2008]. Genus *Caenolestes* O. Thomas, 1895. Pp. 120–124 in Mammals of South America, Volume 1: marsupials, xenarthrans, shrews, and bats (A. L. Gardner, ed.). University of Chicago Press, Chicago, Illinois.

TRIBE, C. J. 1990. Dental age classes in *Marmosa incana* and other didelphoids. Journal of Mammalogy 71:566–569.

VAN NIEVELT, A. F. H., AND K. K. SMITH. 2005. Tooth eruption in *Monodelphis domestica* and its significance for phylogeny and natural history. Journal of Mammalogy 86:333–341.

VIDIGAL, V. C. S., AND J. L. PATTON. 1996. Determination of dental age classes in Amazonian woolly mouse opossums, with notes on intergeneric-variation. Berkeley McNair Journal, University of California, Berkeley, Winter 1996, 4:82–93.

VOSS, R. S., AND S. A. JANSA. 2003. Phylogenetic studies on didelphid marsupials II. Nonmolecular data and new IRBP sequences: separate and combined analyses of didelphine relationships with denser taxon sampling. Bulletin of the American Museum of Natural History 276:1–82.

Submitted 11 July 2012. Accepted 28 January 2013.

Associate Editor was Neal Woodman.

APPENDIX I

Specimens of caenolestid (Paucituberculata, Caenolestidae) marsupials analyzed in this study with localities, geographic coordinates (when available), and specimen numbers. Museum and collection acronyms are: AMNH—American Museum of Natural History, New York, New York, United States; BMNH—British Museum of Natural History, London, United Kingdom; FMNH—Field Museum of Natural History, Chicago, Illinois, United States; IEEUACH—Instituto de Ecología y Evolución, Universidad Austral de Chile, Valdivia, Chile; MACN—Museo Argentino de Ciencias Naturales "Bernardino Rivadavia," Buenos Aires, Argentina; USNM—United States National Museum, Smithsonian Institution, Washington, D.C., United States.

Lestoros inca.—**Peru.** Junín, Cordillera de Vilcabamba, 11°33′35″S, 73°38′28″W (USNM 582114). Cuzco, Machu Pichu, Ruinas de Cedrobamba, 13°03′23″S, 72°27′35″W (AMNH 42685; FMNH 22439; USNM 194406–194410, 194412, 194413, 194417–194423, 194425–194427); Marcapata, Limacpunco, 13°28′S, 70°55′W (FMNH 75112, 75123, 75587); Ocobamba Valley, Tocopoquén, 12°52′S, 72°22′W (USNM 194430–194435); Torontoy, 13°11′58″S, 72°26′41″W (USNM 194382–194385, 194387–194397, 194399–194404, 194921, 194948); Paucartambo, Puesto de Vigilancia Acjanaco, Trocha Ericsson, 13°11′47,3″S, 71°37′10,7″W (FMNH 169817); Paucartambo, La Esperanza, 13°13′S, 71°25″W (FMNH 174445–174475, 174477, 174479, 174481, 174483, 174485, 174487, 174489); Paucartambo, Pillahuata, km 126–128 road between Paucartambo–Pilcopata, 13°08′S, 71°25′W (FMNH 171816–171820,

172034, 172036, 172038, 172040–172042, 172044, 172046, 172048, 172050, 172052).

Caenolestes caniventer.—**Ecuador.** Provincia del Oro, El Chiral, 3°39′S, 79°43′W (AMNH 47173); Mazán, Azuay, 2°52′S, 79°08′W (BMNH 84.383); Cañar, Chical, 2°24′S, 78°58′W (AMNH 62897); Cañar, Piñango/Pinangu/Pinanguso, 2°26′S, 78°58′W (AMNH 62911, 62916, MACN 25.3). **Peru.** Piura, Huancabamba, Huancabamba, km 30 on road to San Ignacio, 5°15′S, 79°29′W (FMNH 81456–81464).

Caenolestes condorensis.—**Ecuador.** "Achupallas," Cordillera del Cóndor, Morona-Santiago, 3°27′03″S, 78°21′39″W (FMNH 152134).

Caenolestes convelatus.—**Ecuador.** Esmeraldas, El Castillo, 0°10′S, 78°33′W (FMNH 44319); Imbabura, Hacienda La Vega, 5 km ESE San Pedro del Lago, 0°13′S, 78°12′W (FMNH 124620); Pichincha, Saloya ("Galaya") West, 0°18′S, 78°40′W (FMNH 53288).

Caenolestes fuliginosus.—**Ecuador.** Chupitán, Pichincha, geographical coordinates not recorded (BMNH 1954.283); Gualea, Pichincha, northeast side, 00°07′S, 78°50′W (BMNH 1934.9.10.275); M[oun]t Pichincha, geographical coordinates not recorded (BMNH 1954.300, 1954.301, 1954.295-1954.297, 1954.299); Napo, Cerro Antisana, Oriente (FMNH 43164, 43165); n[ea]r Mindo, 00°02′S, 78°48′W (BMNH 1954.282); Pichincha M[oun]t., northeast side, geographical coordinates not recorded (BMNH 1978.2848, 1966.2826, 1924.4.18.11–1924.4.18.17, 1934.9.10.267-1934.9.10.274, 1934.9.10.276-1934.9.10.278); Pichincha, 3.45 km en Lloa, Río Cóndor, Huachana (USNM 513429); Pichincha Volcano, 00°01′S, 79°49′W (BMNH 1954.288, 1954.289, 1954.291-1954.293); Pichincha, above Quito, geographical coordinates not recorded (BMNH 1971.924); Pichincha, n[ea]r Quito, geographical coordinates not recorded (BMNH 1954.294, 1954.298); Pichincha, Pichan, 00°10′S, 78°36′W (BMNH 1954.284, 1954.286, 1954.287).

Caenolestes obscurus.—**Colombia.** Paramo Sonson, Antioquia (USNM 293775); Paramo de Jama (USNM 240286). **Venezuela.** Tachira, 35 km S 22 W de San Cristobal (Buena Vista) (USNM 418564).

Rhyncholestes raphanurus.—**Argentina.** Río Negro Province; Parque Nacional Nahuel Huapi, Puerto Blest, 41°02′S, 71°49′W (MACN 20625). **Chile.** X Región [Continental Chile], 9.4 km NW Antillanca and 7.4 km SE Aguas Calientes, PN Puyehue, 40°45′56.30″S, 72°17′34.08″W (FMNH 124002, 124003, 129827); Comuna Entre Lagos, Puyehue, 40°40′S, 72°37′W (IEEUACH 3998–4000); Comuna Puerto Octay, La Picada, 41°06′S, 72°30′W (BMNH 1975.1723 [4 km east], FMNH 127471–127475, 129823–129825, 129830, 127467–127470; IEEUACH 947–952, 2241–2247, 2249, 2250, 2252, 3576, 3578); Contao, 19.7 km N Río Negro and 26.7 km S Contao 41°56′19″S, 72°42′53″W (FMNH 129831, 129832); Maicolpué, 40°35′47.2″S, 73°44′14″W (FMNH 129828); Osorno, 32 km SSE and Puerto Octay, 14.5 km NNW, 40°40′S, 73°10′W (FMNH 129833); Osorno, 84 km SSE, 32 km ESE from Puerto Octay, 41°40′32″S, 72°37′38″W (FMNH 124004); Río Negro, 11.1 km WNW, 41°58′S, 72°29′W (FMNH 129834, 129836); Río Negro, 12.4 km WNW, 41°56′S, 72°31′W (FMNH 135035, 135036); Refugio Volcán Osorno, 41°04′ S, 72°28′ W (FMNH 50071); Vicente Perez Rosales National Park (IEEUACH 4522). X Región [Chiloé Island], Mouth of Río Inio 43°20′03″S, 74°08′08.5″W (FMNH 22422, 22423); Palomar, Fundo El Venado, 42°03′S, 73°58′W (IEEUACH 1831, 1835); Puerto Carmen 43°08′15″S, 73°46′13″W (IEEUACH 1840).

Specimens not examined.—The following specimens were not directly examined but their external measurements, taken from field catalogs and corresponding specimen tags, were used in the analyses. **Peru.** Paucartambo, Puesto de Vigilancia Acjanaco, Trocha Ericsson, 13°11′47,3″S, 71°37′10,7″W (FMNH 169816); Paucartambo, La Esperanza, 13°13′S, 71°25″W (FMNH 174476, 174478, 174480, 174482, 174484, 174486, 174488); Paucartambo, Pillahuata, km 126–128 road between Paucartambo–Pilcopata, 13°08′S, 71°25′W (FMNH 172033, 172035, 172037, 172039, 172043, 172045, 172047, 172049, 172051, 172053).